Title
MEIKTONS: MIXED STATES OF QUARKS AND GLUONS

Authors
Chanowitz, M.
Sharpe, S.

Publication Date
1982-08-01

Lawrence Berkeley Laboratory
UNIVERSITY OF CALIFORNIA

Physics, Computer Science & Mathematics Division

Submitted for publication

MEIKTONS: MIXED STATES OF QUARKS AND GLUONS

Michael Chanowitz and Stephen Sharpe

August 1982

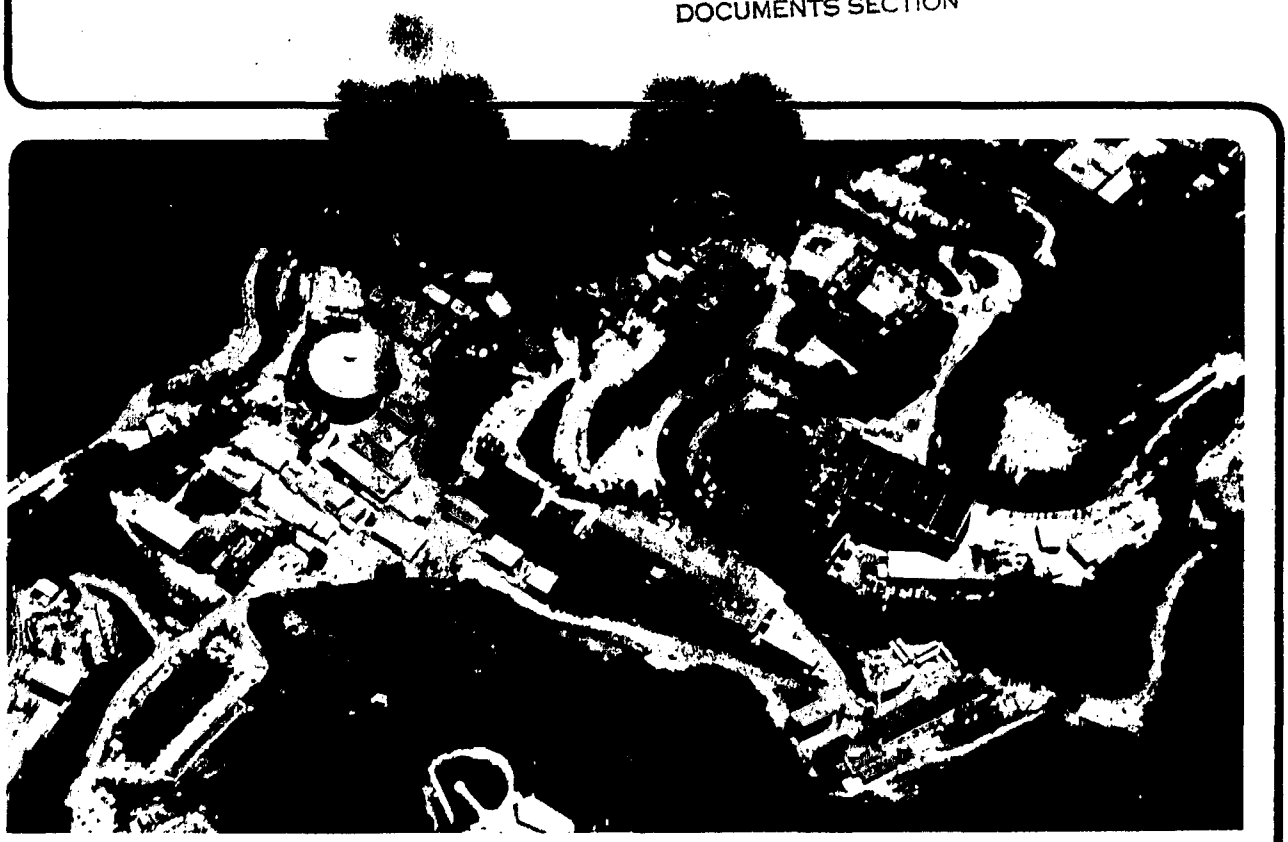

Prepared for the U.S. Department of Energy under Contract DE-AC03-76SF00098

DISCLAIMER

August 1982 LBL-14865

MEIKTONS: MIXED STATES OF QUARKS AND GLUONS*

Michael Chanowitz

and

Stephen Sharpe

Lawrence Berkeley Laboratory
University of California
Berkeley, California 94720

Abstract

We calculate the spectrum of the four ground state meikton ($\bar{q}qg$) nonets, $J^{PC} = (0, 1, 2)^{-+}, 1^{--}$, using the MIT bag model to first order in cavity perturbation theory. Quark and gluon self energies are included by a fit to the s-wave mesons and baryons and to the glueball candidate $\iota(1440)$. We find a large gluon self energy which substantially increases our predictions of the glueball and meikton masses. We discuss the phenomenology of meiktons, including a suggestion that the $A_3(1670)$ and a second peak at 1850 MeV in the $f\pi$ channel may be mixtures of the isovector $\bar{q}q$ d-wave state with the $\bar{q}qg$ s-wave.

*This work was supported by the Director, Office of Energy Research, Office of High Energy and Nuclear Physics, Division of High Energy Physics of the U.S. Department of Energy under contract DE-AC03-76SF00098.

1. Introduction

Though often taken for granted, the existence of valence quarks is a remarkable and poorly understood feature of the meson and baryon spectrum. It is natural to speculate that hadrons also exist which contain valence gluons, and this speculation lies at the heart of bag[1-4] and potential[5,6] model descriptions of the glueball spectrum. In this paper we use the bag model to study another kind of hadron which must exist if valence gluons exist. These are mixed states with valence structure $\bar{q}qg$, which we call meiktons (pronounced "make"-tons), Greek for a mixed object.*

Meiktons have previously been discussed qualitatively[7] and their s-wave spectrum has been studied in the bag model through order α_s.[8-10] Our calculation of the spectrum is also to $O(\alpha_s)$ in the bag model but differs from Refs. 9 and 10 in that we incorporate $O(\alpha_s)$ self energy effects not included by the other authors. As a result our predictions for the meikton (and glueball) masses tend to be substantially larger. The s-wave meikton ground state forms four $SU(3)_{Flavor}$ nonets, $J^{PC} = 1^{--}, (0, 1, 2)^{-+}$ which we expect to lie between 1.2 and 2.5 GeV. We agree with Ref. 10 but not with 9, that the nonets are in order of increasing mass 0^{-+}, 1^{-+}, 1^{--}, 2^{-+}. The 1^{-+} nonet is especially interesting since it is exotic, in the sense that in the nonrelativistic quark model

*We thank the classics scholar M. Whitlock Blundell for suggesting this term. Other classics scholars have instead used the term "hermaphrodite."[7]

no $\bar{q}q$ pair has $J^{PC} = 1^{-+}$.*

Should we expect valence gluons to exist? The question is controversial. The answer may help us to understand why light valence quarks exist and why they obey the OZI rule. Asymptotic freedom[13] and the $1/N_{Color}$[14] expansion both purport to explain these simple features of light quark dynamics but lead to differing expectations on the question of valence glue.

Consider first the $1/N_{Color}$ expansion. OZI violating transitions are suppressed by $1/N^2$ in rate. The probability to create a $\bar{q}q$ pair is $O(1/N)$ so that mixing of the valence $\bar{q}q$ and qqq wave functions with $\bar{q}\bar{q}qq$, $\bar{q}\bar{q}\bar{q}qqq$ ... and $qqqq\bar{q}$, $qqqqq\bar{q}\bar{q}$, ... is suppressed by powers. However in QCD we have only N = 3; also $m_{\eta'} = O(1/N)$[15] but experimentally $m_{\eta'}$ is a typical hadronic mass, an indication that 1/3 can have a coefficient of order 3. In the 1/N expansion there is no suppression of gluon creation and therefore no reason to expect valence gluons. In the framework of the 1/N expansion rising multiplicities cannot be due to creation of $\bar{q}q$ pairs but may reflect multi-glueball production at high energies. This is a striking prediction which can be tested only after we have succeeded in identifying some glueball states.

Another possibility is that perturbation theory already applies in the interiors of ordinary light hadrons, for $r < 1$ fm.[13] Then

*There could however be 1^{-+} $\bar{q}q$ states in the bag model, due to a C-parity doubling that occurs for radial and orbital[11,12] excitations. These are the so-called "spurious" states discussed in Section 2.

the OZI rule and the dominance of the valence wave functions is enforced just by powers of α_s. Until recently it seemed very optimistic to expect α_s to be small enough for this explanation to apply but new results, such as the suggestion of smaller values for Λ[16] and the abruptness of the strong to weak coupling transition[17] seen in lattice calculations, offer at least qualitative support. In this framework the existence of valence gluons is enforced by powers of α_s.

The bag model provides another variant of the perturbation theory explanation. In cavity perturbation theory[18-20] convergence is enforced not by $\alpha_s << 1$ but by small overlap integrals which define the interaction vertices in the cavity. In this framework we also expect valence gluons to exist and be a useful concept.

There are two ways to decide experimentally whether valence gluons exist. One is to find enough of the glueball spectrum to see whether the observed quantum numbers agree with the expectations based on valence gluons. The other, which is the focus of this paper, is to see whether meiktons exist. If there are valence gluons then we are confident that there must be four L = 0 meikton nonets as discussed below.

We use the MIT bag model[18] following the technique of T.D. Lee[19] for perturbation theory in a fixed spherical cavity, as applied to the meson, baryon and glueball spectrum by Barnes, Close, Horgan, and Monaghan.[3,20] The techniques and approximations involved are thoroughly reviewed in Sec. 2. Here we describe the salient differences between our treatment and the others.

First, we take the bag energy density B to be a universal constant, characteristic of all hadrons constructed of quarks and

gluons.* This follows from dynamical models of confinement which give the bag model a natural theoretical basis in QCD. In both the magnetic superconductor ansatz of Nambu, Mandelstam and 't Hooft[21] and the closely related "Princeton bag"[22] based on topological gauge field configurations, the constant B is a property of the complex structure of the QCD vacuum exterior to the hadronic bag while the interior is in the simple perturbative Fock-space ground state.** The QCD vacuum therefore exerts the same inward pressure B on meson, baryon, glueball and meikton bags.

Second, in applying our results we assume that i(1440) is a glueball state but not θ(1640). When θ was discovered in $\psi \to \gamma\eta\eta$ it was suggested that it might be a four quark state with flavor content $\frac{1}{\sqrt{2}}(\bar{u}u + \bar{d}d)\bar{s}s$ and the prediction made that $\Gamma(\theta \to \eta\eta) = \Gamma(\theta \to K^+K^-) >> \Gamma(\theta \to \pi^+\pi^-)$.[23] Recently $\theta \to K^+K^-$ has been observed at a rate consistent with $\Gamma(\theta \to \eta\eta)$ and an upper limit placed on $\Gamma(\theta \to \pi\pi)$ about a factor two below the rates for K^+K^- and $\eta\eta$.[24] This data is consistent with the expectation for a $(\bar{u}u + \bar{d}d)\bar{s}s$ state but is not what we would expect for a glueball.[25]

Third, our calculation incorporates the $O(\alpha_s)$ self energies of the quarks and gluons. This is essential for a consistent perturbative calculation to order α_s and may also have large physical effects, especially for valence gluons. Calculation of the cavity-mode self energies is a formidable, still unsolved

*In this we differ with the treatment of the glueball spectrum in Ref. 3 which relaxes this constraint.

**M.C. wishes to thank Y. Nambu for a discussion of this point.

problem.* In this paper we proceed empirically, using the experimentally observed spectrum to determine the s-wave quark self energy and one combination of gluon mode self energies (the sum of the TE and TM mode self energies). This means that we must redetermine all parameters, such as B and α_s, which we do with a new fit to the meson and baryons, presented in Sec. 3. We find the quark self energy improves the overall fit, especially for the baryon magnetic moments and the Λ-Σ splitting, which were the most serious problems in the original MIT fit.[18]

In Sec. 4 we compare our calculation of the glueball spectrum to previous calculations.[3,4] Here our principal new observation is that if i(1440) is indeed predominantly a glueball, then gluon self energies are very large, several times larger than quark self energies, as might be expected qualitatively given the larger spin and color charge of the gluon. As a result our predictions for the masses of the other glueballs are larger. We find the 2^{-+} glueball at ~ 2.3 GeV. The 2^{++} glueball is about ~ 1 GeV above the 0^{++}; the absolute value of the 0^{++} and 2^{++} masses is very sensitive to the ratio of TE and TM gluon self energies which is not fixed by the i mass alone.

In Sec. 5 these results are applied to the four nonets of the meikton spectrum. The overall mass scale, but not the splittings, depends on the ratio of the TE and TM self energies but much

*The problem has been studied in box-like cavities by Peterson et al.[26] More recently an elegant formulation which may be applicable to practical calculations in spherical cavities has been developed by Hansson and Jaffe.[35]

less sensitively than the 0^{++} and 2^{++} glueballs. We explore values of this ratio from 1/2 to 2. For the smaller value the 0^{-+}, 2^{-+} and 1^{--} meikton nonets tend to lie near $\bar{q}q$ nonets of the same J^{PC}, i.e., the radially excited 0^{-+} nonet, the orbitally excited 2^{-+} nonet, and the orbitally and radially excited 1^{--} nonets.[12] Therefore for small values of the TE-TM ratio we anticipate appreciable mixing with these nonets. Nevertheless even in this case there will be too many states for the $\bar{q}q$ model alone: it is therefore amusing that there may be a peak in the 2^{-+} $f\pi$ channel, at 1850 MeV, just above the $A_3(1670)$.[27] The exotic 1^{-+} nonet might be the easiest to identify as meiktons since there is no $\bar{q}q$ nonet with which it can mix except, possibly, the rather esoteric cavity mode noted above (see footnote on page 3 and the discussion of "spurious" states in Sec. 2 and Ref. 12).

In Sec. 6 we discuss meikton phenomenology. The dominant decays, which are only $O(\alpha_s)$ in the rate, occur when the valence gluon forms a color octet, $J^{PC} = 1^{+-}$ $\bar{q}q$ pair in which either the q or $\bar{q}$ is in a p-wave mode. The cavity then contains two $\bar{q}q$ color octet pairs which, after rearrangement, can fall apart into two $\bar{q}q$ color singlets, the quantum numbers of which determine the dominant two body channels. The only subtlety is the C-parity doubling associated with the so-called "spurious" states discussed in Sec. 2. As discussed there, these configurations may be associated with p-wave excitation of the L = 0 $\bar{q}q$ pair with respect to the cavity. In this case, in addition to the naively expected two body s-wave decays there might also be two body p-wave decays. Many of the experimentally most interesting decay modes are in this latter category.

In Sec. 7 we conclude with some comments on future work, both theoretical and experimental. The possible existence of meiktons increases the complexity of what is already an overwhelmingly rich hadron spectrum between 1 and 2-1/2 GeV. Data of unprecedented high statistics might be needed to expose the structure in this region. The theoretical challenge posed by our empirical determination of the self energies is to actually calculate them in a cavity. Calculations of the quark and gluon self energies would test whether the bag can be a serious quantitative model of hadrons.

In a related paper[28] we have applied the results developed in Sec. 2-5 to the binding of gluinos, the supersymmetric partners of the gluon, into color singlet bound states.

2. The Model and Approximations

In this section we describe the MIT bag model, the approximations to it, and the techniques needed for the calculations presented in the following sections. As discussed above the bag model is well suited for our purposes because it provides a good description of the properties of the lowest lying hadrons and includes valence gluons. Thus, unlike attempts to model valence glue in non-relativistic quark models, we do not have to make any additional ad hoc assumptions--valence gluons come part and parcel of the model.

In the MIT bag model[18] weakly interacting quarks and gluons are confined in a cavity. This "confinement" is produced by giving the inside of the cavity a greater energy density than the vacuum outside. This difference in energy densities is the bag constant, B, which, as discussed in the introduction, we take to be a universal constant. Particles are holes drilled in the vacuum supported against collapse by the pressure of the modes within. Only color singlet combinations of constituents give rise to particles because the color electric fields from a color non-singlet source cannot be confined to a cavity, and thus color non-singlet states have infinite energy.

The MIT bag model is defined by the Lagrangian:[13,29]

$$L = \int_{\text{BAG VOLUME}} \left(i\bar{\psi}_i \not{\partial}_{ij} \psi_j - \frac{1}{4} F^a_{\mu\nu} F^{\mu\nu a} - B \right) - \frac{1}{2} \int_{\text{BAG SURFACE}} \bar{\psi}_i \psi_i \qquad (2.1)$$

where ψ_i is the quark field with i = 1, 2, 3 the color index, $D^\mu_{ij} = \partial^\mu \delta_{ij} - ig A^{\mu a} T^a_{ij}$ is the covariant derivative with T the color

matrices and g the strong coupling constant, $F^a_{\mu\nu} = \partial_\mu A^a_\nu - \partial_\nu A^a_\mu + g f^{abc} A^b_\mu A^c_\nu$ is the gluon field strength with A^b_μ the gluon field and a = 1, ... 8 the adjoint color index, and B is the bag constant. Repeated indices are summed. The equations of motion are that the fields satisfy the coupled Yang-Mills equations inside the cavity and also satisfy the following boundary conditions (n_μ is the unit vector normal to the bag surface):

$$n_\mu F^{\mu\nu}_a = 0 \; ; \; i\not{n}\psi_k = \psi_k \quad , \qquad (2.2a)$$

$$-\frac{1}{2} n_\mu \partial^\mu (\bar{\psi}_i \psi_i) - \frac{1}{4} F_{\mu\nu} F^{\mu\nu} + B = 0 \quad . \qquad (2.2b)$$

Equations (2.2a), which are linear, correspond to requiring no momentum flow across the cavity wall. Equation (2.2b), which is quadratic, ensures that there is no normal component of the force at the boundary. Notice that the quark part of (2.2a) breaks chiral symmetry explicitly.

A complete quantisation of this model has not been accomplished. This is true even for g = 0 because of the non-linear coupling of the fields through the boundary conditions and the motion of the boundary. The standard approximation is to assume a static cavity.[18-20] The linear boundary conditions are enforced on the fields and the cavity modes of the fields are then quantised. The quadratic boundary condition, enforced as a condition on expectation values, is then used to determine the shape and size of the cavity when occupied by any set of modes.

For quarks in a spherical cavity the lowest mode ($L = 0, j = \frac{1}{2}$) is spherically symmetric. Therefore in leading order the s-wave mesons and baryons constructed from this mode satisfy both linear and

quadratic boundary conditions. But quarks with $L \geq 1$ and all gluon modes are not spherically symmetric so that in a spherical cavity they do not satisfy the quadratic boundary conditions. The correct cavity shapes for such modes are not known. Like other authors who have faced this problem,[3,4,9,10,18,20] we use a spherical cavity and only require the pressure to balance globally. This is a better approximation for meiktons than for glueballs because the former contain two L = 0 quarks and only one gluon. Furthermore the important quantities in a bag model calculation are the mode energies and the overlap integrals between various modes, and these appear to be fairly insensitive to the shape of the cavity. For example, the energy of the lowest gluon mode in a sphere and a cube differ by less than 1% for a given cavity volume.[26]

We must also consider states with excited modes. For instance the $J^{PC} = 0^{-+}$ and 2^{-+} glueballs contain one TE gluon and one (excited) TM gluon, and the intermediate states that appear in the meikton calculations contain orbitally and radially excited mesons. For such states the fixed cavity approximation predicts[11] degenerate C-parity partners which are not observed experimentally, e.g., a $J^{PC} = 2^{+-}$ nonet degenerate with the 2^{++} A_2 nonet. It is clear that this prediction is due to the failure to account for the motion of the cavity:* for instance, the four C-parity partners of the usual

*Rebbi[29] and DeGrand[30] include small cavity oscillations, but in an approximation not applicable to mesons and glueballs. They find that the lowest of the extra states is a spurious translation mode while the other extra states exist at higher masses than given by the fixed cavity approximation.

four L = 1 $\bar{q}q$ nonets have precisely the quantum numbers of the two L = 0 $\bar{q}q$ nonets taken in a p-wave with respect to a fixed cavity. It has been suggested[12] that these extra states may exist, but at a higher mass, due to the finite response time of the cavity, and that in the limit of zero response time they would become truly spurious like the spurious states encountered in nuclear physics in the Hartree approximation. Like others before us[2,3] we ignore these states, assuming they have a larger mass if they exist at all. The remaining states we treat in the spherical cavity approximation. An explicit example, for the glueballs, is given in Sec. 4.

Given these approximations we have to quantize QCD in a spherical cavity with the linear boundary conditions on the fields. The quadratic boundary condition is applied only globally which is equivalent to minimizing the energy with respect to the radius R. As shown by T.D. Lee[19] this gives in Coulomb gauge ($\underset{\sim}{\nabla}\cdot\underset{\sim}{A}^a = 0$) the Hamiltonian

$$H = \int_{BAG} d^3x \left(\frac{1}{2}\underset{\sim}{E}^a\cdot\underset{\sim}{E}^a + \frac{1}{2}\underset{\sim}{B}^a\cdot\underset{\sim}{B}^a + \bar{\psi}_i(i\underset{\sim}{\gamma}\cdot\underset{\sim}{\nabla} - m)\psi_i \right. \tag{2.3}$$

$$\left. + g\bar{\psi}_i\underset{\sim}{\gamma}\cdot\underset{\sim}{A}^a T^a_{ij}\psi_j + \frac{g^2}{8\pi}\int_{BAG} d^3y \left(\rho^a(x)\ \Delta^{ab}(x,y)\ \rho^b(y)\right)\right) ,$$

with $\underset{\sim}{E}^a$ and $\underset{\sim}{B}^a$ the usual color electric and magnetic fields, $\underset{\sim}{E}^a$ being transverse, and where the color charge density is:

$$\rho^a = \psi^\dagger_i T^a_{ij}\psi_j - f^{abc}\underset{\sim}{A}^b\cdot\underset{\sim}{A}^c \ , \tag{2.4}$$

and the Coulomb Green function, to order g^2, is:

$$\Delta^{ab}(x,y) = \delta^{ab}\left(\frac{1}{|\underset{\sim}{x}-\underset{\sim}{y}|} - \frac{1}{R} + \sum_{L=1}^{\infty}\left(\frac{L+1}{L}\right)\frac{|xy|^L}{R^{2L+1}}\,P_L(\cos\theta_{xy})\right) . \tag{2.5}$$

The - 1/R in the Coulomb Green function follows from the careful limiting procedure for introducing the cavity used by T.D. Lee. In fact it is gauge variant and gives no contribution to the masses of color singlet states, provided all Coulombic self energy effects are included.

We calculate the spectrum perturbatively using the formalism of Close and Horgan.[20] Thus we expand the fields in normal modes satisfying the linear boundary conditions:

$$\psi^i(x) = \sum_{\substack{\text{Quark}\\ \text{Modes, m}}} U_m(\underset{\sim}{x})\, b_m^i\, e^{-iE_m t} + V_m^*(\underset{\sim}{x})\, d_m^{i\dagger}\, e^{iE_m t} ,$$

$$\underset{\sim}{A}^a(x) = \sum_{\substack{\text{Gluon}\\ \text{Modes, n}}} \underset{\sim}{A}_n(\underset{\sim}{x})\, a_n^a\, e^{-i\omega_n t} + \underset{\sim}{A}_n^*(\underset{\sim}{x})\, a_n^{\dagger a}\, e^{i\omega_n t} . \tag{2.6}$$

where E_m and ω_n are the energies of the quark and gluon modes respectively, and the modes are conventionally normalized:

$$\int d^3x\; U_m^\dagger(x)\; U_{m'}(x) = \delta_{mm'}; \qquad \int d^3x\; \underset{\sim}{A}_n^*(\underset{\sim}{x})\cdot\underset{\sim}{A}_{n'}(\underset{\sim}{x}) = \frac{1}{2\omega_n}\,\delta_{nn'} . \tag{2.7}$$

The creation and annihilation operators appearing in the expansion satisfy canonical commutation relations. The Hamiltonian is expressed as a free and interacting part:

$$H = H(g=0) + H_{INT} , \tag{2.8}$$

$$H(g=0) = \sum_{\substack{\text{Quark}\\ \text{Modes, m}}} E_m\left(b_m^{i\dagger}b_m^i - d_m^i d_m^{i\dagger}\right) ,$$

$$+ \sum_{\substack{\text{Gluon}\\ \text{Modes, n}}} \frac{\omega_n}{2}\left(a_n^{a\dagger}a_n^a + a_n^a a_n^{a\dagger}\right) .$$

Finally the energy of a mode in time ordered perturbation theory is:

$$H_0|m> = E_m|m> ,$$

$$E = E_m + <m|H_I|m> + \sum_p \frac{<m|H_I|p><p|H_I|m> + \ldots}{E_m - E_p} . \tag{2.9}$$

In order to build states we will use the L = 0, J = $\frac{1}{2}$ quark modes given by (we follow closely the notation of Ref. 20):

$$U_s(\underset{\sim}{x}) = N_s\begin{pmatrix} j_0(k_s r/R)\; u \\ i\,\dfrac{k_s}{E+mR}\, j_1(k_s r/R)\; \underset{\sim}{\sigma}\cdot\hat{\underset{\sim}{x}}\; u \end{pmatrix}$$

$$N_s = \frac{1}{\sqrt{4\pi}}\;\frac{k_s}{j_0(k_s)\;\sqrt{2E(E-1)+mR}} , \tag{2.10}$$

with $E = \sqrt{k_s^2 + m^2R^2}$ the energy in units of R^{-1}, R the cavity radius, $r = |\underset{\sim}{x}|$, and u a two component spinor. The dimensionless momentum k_s is determined by the linear boundary condition:

$$j_0(k_s) = \frac{k_s}{E+mR}\; j_1(k_s) . \tag{2.11}$$

For m = 0 the lowest mode has $E = k_s = 2.04$. We shall also use both the lowest transverse electric (TE) and transverse magnetic (TM) gluon modes. The lowest gluon mode is the $J^{PC} = 1^{+-}$ TE model (we use the notation of Ref. 3):

$$\underset{\sim}{A}_m^{TE}(\underset{\sim}{x}) = \alpha^{TE}\, j_1(\omega r/R)\sqrt{\frac{3}{8\pi}}\;\hat{\underset{\sim}{x}} \times \underset{\sim}{e}_m$$

$$\alpha^{TE} = 1/\left(j_0(\omega)\sqrt{\omega(\omega^2 - 2)}\right)$$

$$j_0(\omega) = j_1(\omega)/\omega \implies \omega = 2.74 \quad , \tag{2.12}$$

where $\underset{\sim}{e}_m$, m = -1, 0, +1, are the unit spherical vectors. The lowest TM mode is the 1^{--} mode:

$$\underset{\sim}{A}_m^{TM}(\underset{\sim}{x}) = \frac{\alpha^{TM}}{\sqrt{24\pi}}\left(2j_0(\omega r/R)\underset{\sim}{e}_m + 3\, j_2(\omega r/R)\left(\hat{\underset{\sim}{x}}\,\hat{\underset{\sim}{x}}\cdot\underset{\sim}{e}_m - \frac{1}{3}\underset{\sim}{e}_m\right)\right)$$

$$\alpha^{TM} = 1/\left(j_0(\omega)\sqrt{\omega}\right)$$

$$j_1(\omega) = 0 \implies \omega = 4.49 \quad . \tag{2.13}$$

Notice that the least energetic mode has positive parity. This has important consequences for the quantum numbers of the lowest meikton states. We also need p and d quark modes for the intermediate states, and these are given in the appendix.

We now have all the ingredients for a bag model calculation in the static spherical cavity approximation. To find the mass of a state we must minimize its energy as a function of its radius. The energy consists of the following parts which we now discuss:

(a) volume energy, (b) zero-point energy, (c) mode energies, (d) perturbative energy corrections, and (e) the localization energy.

(a) The volume energy is

$$E = \frac{4\pi}{3} R^3 B \quad , \tag{2.14}$$

where B is the bag constant which, as discussed in the introduction, we take to be universal. The value of B is determined by the fit to the mesons and baryons described in Sec. 3.

(b) The zero point energy is:

$$E = \sum_{\text{Quark Modes, m}} - E_m + \sum_{\text{Gluon Modes, n}} \frac{\omega_n}{2} \quad . \tag{2.15}$$

Using Green function methods Bender and Hays[31] and, more recently, Milton[32] showed that for a spherical cavity the form of the self energy is

$$E = Z_4\Lambda^4 R^3 + Z_2\Lambda^2 R + Z_0 R^{-1} + O(\Lambda^{-1}) \tag{2.16}$$

with Λ a cut-off. The Z_4 term (the usual energy density divergence) can be absorbed into a renormalization of the bag constant. But the Z_2 term requires the introduction of a perimeter term into the bag action and therefore an extra parameter to be fit. We do not include this extra parameter because we can obtain a very good fit without it.

The Z_0/R term is important to obtain a good fit. Milton,[32] using the same approximation as that which allowed extraction of the quadratic divergence, found a finite contribution to Z_0 of $\sim .3$. But he, and Bender and Hays,[31] noticed that there may also be logarithmically divergent contributions to Z_0, in which case Z_0 becomes an arbitrary renormalized parameter.* Furthermore there are other contributions to

*Also there could be $\ell nR/R$ terms in the energy in this case.

the energy with the same form--the perturbative vacuum energy and the localisation energy. The former has not been calculated and the latter can only be roughly estimated, as discussed below. For all these reasons we cannot predict Z_0. As in the original papers[18] we determine it empirically from the fit in Sec. 3.

(c) The mode energies are obtained from the eigenvalue conditions given above, and lead to:

$$E_{Mode} = \left(\sum_{\substack{\text{Quarks \&} \\ \text{Antiquarks}}} E_m + \sum_{\text{Gluons}} \omega_n \right) / R \quad . \tag{2.17}$$

(d) The perturbative energy corrections are obtained using Eq. (2.9). We work to first order in $\alpha_s = g^2/4\pi$, and we find, as with all bag model fits, a large value for α_s: $2 \lesssim \alpha_s \lesssim 3$. This is because each power of α_s comes with overlap integrals (the matrix elements in (2.9)) and an energy denominator, both of which numerically reduce the correction. Thus the effective expansion parameter is much smaller than α_s and we expect the higher order corrections to be small. This expectation is supported by explicit $O(\alpha_s)$ calculations of the corrections to magnetic moments, charge radii and axial charges of the nucleons.[33]

In a standard way Eq. (2.9) can be represented diagrammatically with the matrix elements becoming vertices. The vertices which we need are shown in Table 1,* where we have shown the coefficients in H_I of the appropriate creation and annihilation operators. Parity conservation restricts the number of vertices, e.g., s-quark → s-quark + TM-gluon is not allowed. The dimensionless L and C factors depend

*We have not included many of the vertices necessary for the calculation of the energy shifts in glueballs as they are not necessary for meiktons and have been discussed fully elsewhere.[3,4]

on the masses of the participating quarks through the combination mR. Our best fits have massless up and down quarks and a strange quark mass such that $1.75 \lesssim m_s R \lesssim 2.25$. Thus we give values of the L factors for mR = 0 and 2. In Appendix 1 we give expressions for them, as well as the relationship of our definitions to those of other authors. Many of these vertices have been previously calculated,[20,34] though in nearly all cases only for massless quarks, and we have checked agreement in these cases.

These vertices are used to construct exchange and self energy diagrams. The exchange diagrams (e.g. Fig. 2) involve only intermediate states with a restricted range of angular momenta, but all radial excitations contribute. However, except in one case discussed in Sec. 5, the contribution of the radial excitations is only a few percent of that of the lowest intermediate state and we will ignore it. The Green function methods used by various authors[4,11,18] sum the contribution from all the radial excitations.

The self energy graphs for quarks and gluons are shown in Fig. 1. Orbital and radial excitations are present in the intermediate states; the orbital excitations lead to ultraviolet infinities. Because they are short distance singularities they are independent of the size and shape of the cavity, and in fact they correspond exactly to the mass renormalization infinities in unconfined perturbation theory.* But there is no mass renormalization in confined perturbation theory for gluons and massless quarks because of gauge and chiral symmetries respectively. Thus these infinities are absent in self energy graphs in a cavity, although there are finite terms proportional to 1/R because

*A careful study of this point has been made in Ref. 35.

the low frequency modes in the cavity differ from those of unconfined perturbation theory. These finite terms will be different for each mode. They are calculable, though the calculations are difficult and have not yet been done. Thus we parameterize the self energies as

$$\Delta E_{\text{Self Energy}} = \alpha_s \, C_i/R \qquad i = Q(\text{s-quark}),\ TE,\ TM \tag{2.18}$$

and fit them.

For massive quarks there is an infinity in the self energy graphs which corresponds to the logarithmically divergent mass in unconfined perturbation theory. This must be renormalized as usual and leads to the following self energy:[35]

$$\Delta E_{\text{Self Energy}} = \alpha_s \left(\frac{C(mR,\ \ell n \Lambda^2/m^2)}{R} + m\delta \frac{\partial E_{\text{mode}}}{\partial m} \right), \tag{2.19}$$

where the first term comes from the $O(\alpha_s)$ diagrams evaluated with a cut-off Λ, and the second is the counterterm with δ dimensionless. The counterterm includes the factor $\partial E_{\text{mode}}/\partial m$ because we are considering the self energy of a mode rather than a free particle. Hannson and Jaffe[35] have shown that the first term can be written as:

$$\frac{C(mR,\ \ell n \Lambda^2/m^2)}{R} = \frac{1}{\pi} m \ \ell n \frac{\Lambda^2}{m^2} \frac{\partial E_{\text{mode}}}{\partial m} + \frac{C'(mR)}{R}$$

$$= \frac{1}{\pi} m \left(\ell n \frac{\Lambda^2}{\mu^2} + \ell n \frac{\mu^2}{m^2} \right) \frac{\partial E_{\text{mode}}}{\partial m} + \frac{C'(mR)}{R} \tag{2.20}$$

where C' is finite, μ^2 is arbitrary, and the fact that the divergent term is proportional to $\partial E_{\text{mode}}/\partial m$ for any mode is crucial for renormalizability, since one infinite counterterm can then remove the divergence from all quark mode energies. Absorbing the divergence into δ gives for the total self energy:

$$\Delta E_{\text{Self Energy}} = \frac{\alpha_s}{R} \left(C'(mR) + mR \left(\frac{1}{\pi} \ell n \frac{\mu^2}{m^2} + \delta' \right) \frac{\partial E_{\text{mode}}}{\partial m} \right) \tag{2.21}$$

$$\equiv \frac{\alpha_s}{R} \ C''(mR,\ \ell n \frac{\mu^2}{m^2},\ \delta') \quad ,$$

where all quantities are finite and $C'(0) = C''(0) = C_Q$. There remains the freedom of finite renormalization parameterized by δ' and μ^2 (which are not independent) and we choose δ' such that at typical values of mR, i.e. $mR \sim 2$, $C'' = C_Q$ for the s-quark mode. Then to the extent that we can ignore the variation of C''(mR) with mR for $mR \sim 2$ the self energy of a strange s-quark in a cavity of the sizes we consider is the same as for a massless quark, and we need not introduce new parameters to describe this variation. By considering the variation of typical quantities (e.g. the mode energies) with mR we estimate the effect of this approximation to be 10 MeV or less.

(e) Bag model states are localized in space, and thus they must represent approximations to wave packets of the hadrons which they are modeling. These wave packets will have $\langle \underset{\sim}{p}_{\text{hadron}} \rangle = 0$ since the bag is fixed, but because of the uncertainty principle $\langle \underset{\sim}{p}^2_{\text{hadron}} \rangle$ must be nonzero. Thus the mass that we obtain from a bag model calculation is really the average energy of the wave packet, i.e.

$$m_{\text{bag}} = \left\langle \sqrt{m^2_{\text{hadron}} + \underset{\sim}{p}^2_{\text{hadron}}} \right\rangle \quad . \tag{2.22}$$

The real hadron mass is thus less than the bag mass because of the localisation energy. Furthermore the static properties of the states are altered and this will be discussed in the next section. For a thorough review of these issues see Ref. 36.

In general the localisation energy will most effect the lightest states, the details depending on the chosen model for the wave packet. For heavy states Eq. (2.19) can be expanded giving:

$$m_{bag} \simeq m_{hadron} + \frac{\langle \underset{\sim}{p}^2_{hadron} \rangle}{2m_{hadron}} , \qquad (2.23)$$

$$= m_{hadron} + \frac{x_{hadron}}{R^2} .$$

For any reasonable choice of wave packet, and whether one minimizes m_{bag} or m_{hadron}, the effect of this extra term can be imitated by redefinitions of Z_0, C_Q and m_s, with the main effect being on Z_0.[36]

Thus the pseudoscalar mesons will be most effected by the localisation energy but in a way which depends crucially on the choice of wave packet. Because of this and the problem of chiral symmetry and the U(1) problem we exclude the pseudoscalars from our fit. For the rest of the spectrum localisation effects should be adequately represented by the parameters Z_0, C_Q and m_s.

3. New Fits to s-wave Mesons and Baryons

In previous bag model fits to the mesons and baryons[18] the effect of $O(\alpha_s)$ self energy diagrams were not systematically included. We include these diagrams by introducing another parameter, the quark self energy, and therefore must perform a new fit to determine the best values of all the parameters. We are able to improve significantly on the earlier fits. For reasons discussed at the end of Sec. 2 we do not attempt to fit the $J^P = 0^-$ mesons (although we do report their masses as predicted by each fit).

The energy of a given state is

$$E = \frac{4\pi}{3} R^3 B + \frac{Z_0}{R} + \sum_{\text{constituents}} \frac{E_{mode}}{R} + \Delta E \qquad (3.1)$$

where ΔE is the $O(\alpha_s)$ contribution coming from the diagrams shown in Fig. 2. For mesons this is

$$\Delta E = \frac{\alpha_s}{R} \left(\frac{4}{3} \langle \underset{\sim}{S}_q \cdot \underset{\sim}{S}_{\bar{q}} \rangle \frac{L^{ssE}(m_q R) L^{ssE}(m_{\bar{q}} R)}{\omega_{TE}} - \frac{4}{3} C^{ss}(m_q R, m_{\bar{q}} R) + 2C_Q \right) , \qquad (3.2)$$

where the three terms are, respectively, the transverse exchange, Coulomb exchange and self energy contributions. $\frac{4}{3}$ is the color factor, and $\underset{\sim}{S}_q$ and $\underset{\sim}{S}_{\bar{q}}$ are the quark and antiquark spin matrices and m_q and $m_{\bar{q}}$ are their masses. For baryons the $O(\alpha_s)$ contribution is, using the same format,

$$\Delta E = \frac{\alpha_s}{R}\left(\sum_{\substack{\text{pairs of}\\ \text{quarks}}} \frac{2}{3}\left(\langle \underset{\sim}{S}_{q_1} \cdot \underset{\sim}{S}_{q_2} \rangle \frac{L^{ssE}(m_{q_1}R) L^{ssE}(m_{q_2}R)}{\omega_{TE}} \right.\right. \tag{3.3}$$

$$\left.\left. - C^{ss}(m_{q_1}R, m_{q_2}R)\right) + 3\, C_Q \right),$$

where $\langle \underset{\sim}{S}_{q_1} \cdot \underset{\sim}{S}_{q_2} \rangle$ is evaluated in the SU(6) wavefunction.[18] The only spin dependence comes from the transverse exchange terms but the Coulomb exchange and self energies do contribute to the baryon-meson splitting. Because the L and C factors depend in a complicated way on the quark masses we have minimized the energy numerically.

The parameters to be fitted are B, Z_0, $m_u = m_d$ (we ignore isospin splittings), m_s, α_s and C_Q. We have searched for fits which give all the vector mesons and the baryon octet and decuplet within 25 MeV. We used 25 MeV because it is small on the scale of the splittings within multiplets but large enough that bag model fits, though not too many, do exist, and because we make no claim of greater accuracy for the model. We find such fits for $m_u = m_d = 0$ but none for $m_u = m_d = 50$ MeV. For $m_u = m_d = 0$ we find a cigar shaped range of fits falling close to the straight line segment in parameter space running between:

$$\begin{array}{rcccr} 150\ \text{MeV} & > & B^{1/4} & > & 120\ \text{MeV} \\ -2.1 & > & Z_0 & > & -2.9 \\ 2.0 & < & \alpha_s & < & 2.8 \\ .22 & < & C_Q & < & .48 \end{array}$$

with $m_s \cong .33 - .35$ for the smaller values of α_s, and $m_s \cong .33 - .37$ for larger values. Two fits are shown in Table 2, together with the

original MIT fit. We show one fit with $\alpha_s = 2.2$ (fit I) in order to compare with the original MIT fit,[18] while the other (fit II) has $\alpha_s = 2.8$ and is our best fit. The MIT fit does not include self energies except for the coulomb diagrams with the lowest intermediate quark states (see Fig. 2) and these behave like a positive contribution to the quark mass. Thus the MIT fit gives a smaller m_s.

The table shows that we have been able to obtain good overall fits. Fit I and the original MIT fit are of comparable quality, but fit II shows a significant improvement, differing by at most 16 GeV from the experimental masses. The "predictions" for the pseudoscalar mesons are of course poor though it is perhaps surprising how well the kaon is fit. The quark self energy parameter C_Q varies in the fits from roughly a third to a half of the mode energy. Two of the most serious problems of the original MIT fit were the splitting between the Λ and Σ and the overall scale of the baryon magnetic moments. For both of these fit I is only marginally better, but fit II is significantly better. For the Λ-Σ splitting the MIT fit gave 39 MeV, fit I gives 48 MeV and fit II gives 60 MeV as compared to the experimental splitting of 77 MeV. For the baryon magnetic moments it is the larger radii in fit II which give the improvement, though the scale of the magnetic moments is still ~10% too low. This is shown in column (a) of Table 3. The ratios of the magnetic moments were reasonably well accounted for by the MIT fit and are changed little by our new fits. Details of the calculation of magnetic moments can be found in Ref. 18 which also includes a discussion of other predictions, e.g. axial vector coupling constants, which are improved little by our new fits.

We have verified that the improvements are in fact due to the

nonzero self energy by searching for fits with $C_Q = 0$. We find that there are no fits with the L = 0 vector mesons and baryons all within 25 MeV of their experimental values nor with the Λ-Σ mass splitting greater than 40 MeV. The nucleon radius in the best of these fits is very small, $\lesssim 4\ \text{GeV}^{-1}$, which implies a very small proton magnetic moment, $\mu_p \lesssim 1.5$, almost 50% below the experimental value of 2.79.

The predictions of the static bag model are altered when account is taken of the momentum spread of the hadron wave packet discussed in Sec. 2. In the limit $\langle p^2_{\text{hadron}} \rangle \ll m^2_{\text{hadron}}$ Donoghue and Johnson[36] found for the magnetic moment

$$\mu = \mu_{\text{static bag}} \left(1 + \frac{1}{2} \frac{\langle p^2_{\text{hadron}} \rangle}{m^2_{\text{hadron}}} \right) . \qquad (3.4)$$

This effect increases the magnetic moments and, using Donoghue and Johnson's model for the wave packet which has $\langle p^2_{\text{hadron}} \rangle \sim 10/R^2$, the results shown in column b of Table 3 are obtained. Fit II is still preferred, but the difference between fit II and the MIT fit is reduced. Of course the results depend on the model for the wave packet chosen.

4. Glueballs

Using the parameters determined in Sec. 3 we will now consider the glueball spectrum. In particular we use the glueball candidate i(1440) to learn about the gluon self energies and thus about the mass scale of states containing valence glue.

The quantum numbers of the glueballs in the static spherical cavity approximation to the bag model have been discussed in detail.[1,2] We briefly review the results here. The lowest lying states (before inclusion of $O(\alpha_s)$ effects) are constructed of two TE(1^{+-}) modes and thus have $J^{PC} = 0^{++}$ and 2^{++}, the spin 1 state being forbidden by Bose statistics.

The first orbitally excited states are constructed from either a TE mode and a TM(1^{--}) mode or from a TE mode and an orbitally excited TE mode with $J^{PC} = 2^{--}$. The former combination gives $J^{PC} = (0, 1, 2)^{-+}$ and the latter $J^{PC} = (1, 2, 3)^{-+}$. It is here that we encounter the so-called "spurious" states discussed in Sec. 2. Four of these six states have the quantum numbers of the ground state, $(0, 2)^{++}$, moving in a p-wave with respect to the cavity: 1^{-+} and $(1, 2, 3)^{-+}$. These are the "spurious" states which we (following Donoghue, Johnson, and Li[2]) discard, leaving just the doublet $(0, 2)^{-+}$. However, as discussed in Sec. 2, the real nature of the "spurious" states is a difficult problem, beyond the scope of this paper.

At "zeroeth" order* in α_s with the MIT values for B and Z_0, the $(0, 2)^{++}$ states have a mass of .96 GeV and the $(0, 2)^{-+}$ states weigh 1.29 GeV.[1,2] Using our fits we find slightly lower "zeroeth" order

*This is not really zeroeth order in α_s because Z_0 contains vacuum bubble contributions of $O(\alpha_s)$.

masses. However, this pattern of states is grossly altered by the $O(\alpha_s)$ contribution to the energy, the effect being greater than for the mesons and baryons mainly because of the larger color and spin Casimir operators associated with the glueball diagrams. These diagrams are shown in Fig. 3. All but the self energy diagrams have been calculated by Barnes et al.,[3] using the same methods as in this paper and more recently by Carlson et al.[4] who used Green function methods.* We have checked the calculations and are in substantial agreement with both papers (including the erratum of Ref. 3). The very small discrepancies we find are chiefly attributable to the numerical integrations and, in the case of Ref. 4, to their use of the Green function method. By a Fierz transformation (see Appendix 2) we have resolved the apparently large discrepancy between Refs. 3 and 4 for the $(TE)^2(TM)^2$ vertex. We then find that we and Refs. 3 and 4 are in agreement on the spin dependent part; we also agree with Ref. 3 on the spin independent part, which was not calculated in Ref. 4. In addition we do have small differences with Ref. 3 due to their omission of the TE 2^{--} exchange graph (Fig. 3) and of radially excited TE mode exchanges.

Our results are that the coefficients of α_s/R from the exchange diagrams are for the 0^{++}, 2^{++}, 0^{-+}, 2^{-+} glueballs respectively -2.50, .20, -2.54, -.05. The self energy contributions are 2 C_{TE} for the $(0, 2)^{++}$ states and $C_{TE} + C_{TM}$ for the $(0, 2)^{-+}$ states.

Without knowing the gluon self energy parameters we cannot make predictions for states with valence glue. We shall identify the i(1440) state seen in J/ψ radiative decay with the 0^{-+} glueball. The evidence

*The transverse gluon exchange diagrams are also calculated by Konoplich and Schepkin[37] with results in agreement with Ref. 3.

for this has been discussed in detail elsewhere.[23,38] We do not however assume that $\theta(1640)$ is a glueball, as the recently reported measurement of $\theta \to K^+K^-$ and bound on $\theta \to \pi\pi$[24] is not what we would expect for a glueball but does agree with the prediction[23,25] for a four quark state, $1/\sqrt{2}\ (\bar{u}u + \bar{d}d)\bar{s}s$. Given these assumptions we can find $C_{TE} + C_{TM}$ for each of our previous fits. This in turn allows a prediction of the 2^{-+} glueball mass. The 0^{++} and 2^{++} glueball masses depend in addition on the ratio C_{TE}/C_{TM}. Assuming 1/2, 1 and 2 for this ratio we obtain the predictions shown in Table 4.

There are a number of points to notice. First, the 0^{++} and 2^{++} glueball masses are very sensitive to the ratio of the TE and TM self energies while the 2^{-+} glueball mass is independent of this ratio. Second, the gluon self energies required by the fits are very large--the average of C_{TE} and C_{TM} is ~ 1.8 for fit I and ~ 2.7 for fit II. The origin of this is clear. The 0^{-+} glueball weighs about 1 GeV at "zeroeth" order but then receives a large negative $O(\alpha_s)$ exchange energy. In order to bring it up to a mass of 1.44 GeV a large positive self energy contribution is required. The large gluon self energy raises our predicted glueball spectrum significantly relative to the predictions of other authors.[2,3] In particular the 0^{++} glueball is sufficiently massive that vacuum mixing effects may not be as large as seems necessary when self energies are neglected and the 0^{++} state becomes tachyonic.[26,30] Finally notice that the predicted masses, though not the radii, are almost independent of which fit is used.

Clearly more theoretical and experimental work are required. On the theoretical side the self energies must be calculated and the accuracy of the static spherical cavity approximation established.

If these results are satisfactory the next step will be to compute the $O(\alpha_s^2)$ corrections to see if there is truly a convergent expansion: this is essential given the very large value of $C_{TE} + C_{TM}$ from our fits. Experimentally more evidence is needed on the nature of i(1440) and for other glueballs. Because of the uncertainties we have not made predictions for other glueball states, e.g., radial excitations or three gluon states. Our results show that the $O(\alpha_s)$ corrections--and particularly the self energies--may have a profound effect on the glueball spectrum.

5. The Meikton Spectrum

We are now in a position to predict the meikton masses. We will only consider the lowest lying states. These are constructed from an $s_{1/2}$ quark and an $s_{1/2}$ antiquark combined in a $\bar{q}q$ color octet with $J^{PC} = 0^{-+}$ or 1^{--}, and a TE gluon with $J^{PC} = 1^{+-}$. The result is four $\bar{q}qg$ flavour nonets with $J^{PC} = 1^{--}$, $(0, 1, 2)^{-+}$.

At "zeroeth" order the energy of the meiktons is

$$E_0 = \frac{4\pi}{3} R^3 B + \frac{(E_{quark} + E_{antiquark} + \omega_{TE} + Z_0)}{R} \qquad (5.1)$$

and the nonets are ideally mixed and degenerate. The meiktons without strange quarks have masses in GeV. of 1.09 (fit I), .91 (fit II), or 1.21 (MIT fit). For comparison, the non-strange baryon masses in this approximation are .96 (fit I), .71 (fit II), or 1.08 (MIT). For each strange quark the mass increases by about 150 MeV. The meiktons are heavier than the baryons because the TE gluon mode energy (2.74/R) is greater than that of an $s_{1/2}$ quark (2.04/R). This difference is increased at $O(\alpha_s)$ because the gluon self energy is greater than that of the quark.

The $O(\alpha_s)$ diagrams are shown in Fig. 4. Only graphs (a, b, c, e) were included in Ref. 10. Diagrams (a)-(d) are the usual transverse and Coulomb exchange graphs. The Compton [(e), (f) and (g)] and Z-graphs [(h), (i)] occur uniquely in meiktons because meiktons have both quark and gluon constituents. Notice that the Compton graphs can have an intermediate $d_{3/2}$ quark or radially excited $s_{1/2}$ quark and that the Z-graphs involve intermediate p quarks. The s-channel transverse (j) and Coulomb diagrams (k) are also unique to meiktons because the quark and antiquark are in a color octet; they contribute

to meiktons in which the $\bar{q}q$ pair is a flavor-singlet spin-triplet. Finally, diagram (1) shows the self energy graphs.* With the exception of graph (g) which is discussed below, diagrams with radially excited modes in the intermediate state contribute at most 5 MeV to the mass of the meiktons and we do not include them in our result.

*There is a subtlety associated with the fermion loop contribution to the gluon self energy (see Fig. 1). When one of the fermions in the loop is an $s_{1/2}$ quark (or antiquark) fermi statistics requires it to have different quantum numbers from the $s_{1/2}$ quark already present in the meikton. This constraint does not apply to the high spin intermediate states which are responsible for the divergences, and so the gluon self energy in meiktons differs from that in mesons and baryons by a finite calculable amount. This is, however, the same as the effect discussed for Z-graphs in the text, and it is easy to show that the contribution from the excluded intermediate states in the two cases exactly cancel, so that the constraints due to fermi statistics could be ignored. (SS thanks R. Jaffe for pointing out this "cancellation" of constraints.) These constraints are in any case phenomenologically unimportant, since their effect on the gluon self energy and the Z-graphs is ~ 1 MeV.

Calculation of these diagrams gives the energy shift:

$$\Delta E = \frac{\alpha_s}{R}\left(\Delta E_A + \Delta E_B\right), \tag{5.2}$$

$$\Delta E_A = -\frac{1}{3}\langle \underset{\sim}{S}_q \cdot \underset{\sim}{S}_{\bar{q}}\rangle \frac{L^{ssE}(m_q R) L^{ssE}(m_{\bar{q}} R)}{\omega_{TE}} + \frac{1}{6} C^{ss}(m_q R, m_{\bar{q}} R) \tag{5.3}$$

$$+ \left[\left(6\langle \underset{\sim}{S}_q \cdot \underset{\sim}{S}_g\rangle \frac{L^{ssE}(m_q R) L^{EEE}}{\omega_{TE}} - \frac{3}{2} C^{sE}(m_q R)\right) + q \leftrightarrow \bar{q}\right]$$

$$+ \left[\left(\frac{1}{3}\left(1 - 2\langle \underset{\sim}{S}_q \cdot \underset{\sim}{S}_g\rangle\right) + \frac{1}{24}\left(1 + 2\langle \underset{\sim}{S}_q \cdot \underset{\sim}{S}_g\rangle\right)\right) \frac{L^{ssE^2}(m_q R)}{\omega_{TE}} + q \leftrightarrow \bar{q}\right]$$

$$+ 2\, C_q + C_{TE},$$

$$\Delta E_B = \left[\left(-\frac{8}{9}\left(1 + \langle \underset{\sim}{S}_q \cdot \underset{\sim}{S}_g\rangle\right) \frac{L^{sdE}(m_q R)^2}{E_{d_{3/2}} - E_s - \omega_{TE}}\right.\right. \tag{5.4}$$

$$\left.\left. + \frac{1}{9}\left(1 - \langle \underset{\sim}{S}_q \cdot \underset{\sim}{S}_g\rangle\right) \frac{L^{sdE}(m_q R)^2}{E_{d_{3/2}} - E_s + \omega_{TE}}\right) + q \leftrightarrow \bar{q}\right]$$

$$+ \left[\left(-\frac{1}{3}\left(1 - 2\langle \underset{\sim}{S}_q \cdot \underset{\sim}{S}_g\rangle\right) \frac{L^{ss'E}(m_q R)^2}{E_{s'} - E_s - \omega_{TE}}\right.\right.$$

$$\left.\left. + \frac{1}{24}\left(1 + 2\langle \underset{\sim}{S}_q \cdot \underset{\sim}{S}_g\rangle\right) \frac{L^{ss'E}(m_q R)^2}{E_{s'} - E_s + \omega_{TE}}\right) + q \leftrightarrow \bar{q}\right]$$

$$+\left\{\left\{-\frac{1}{24}\left(\frac{7}{8}+2\langle \underset{\sim}{S}_q\cdot\underset{\sim}{S}_g\rangle\right)\frac{L^{spE}(m_qR)^2}{E_{P_{1/2}}+E_s-\omega_{TE}}\right.\right.$$

$$\left.\left.+\frac{1}{3}\left(\frac{7}{8}-2\langle \underset{\sim}{S}_q\cdot\underset{\sim}{S}_g\rangle\right)\frac{L^{spE}(m_qR)^2}{E_{P_{1/2}}+E_s+\omega_{TE}}\right\}+q\leftrightarrow\bar{q}\right\}$$

$$+\left\{\left\{-\frac{1}{12}\left(\frac{7}{8}-\langle \underset{\sim}{S}_q\cdot\underset{\sim}{S}_g\rangle\right)\frac{L^{sp'E}(m_qR)^2}{E_{P_{3/2}}+E_s-\omega_{TE}}\right.\right.$$

$$\left.\left.+\frac{2}{3}\left(\frac{7}{8}+\langle \underset{\sim}{S}_q\cdot\underset{\sim}{S}_g\rangle\right)\frac{L^{sp'E}(m_qR)^2}{E_{P_{3/2}}+E_s+\omega_{TE}}\right\}+q\leftrightarrow\bar{q}\right\}$$

$$+\frac{\delta^{IO}}{2}\left(\frac{3}{8}+\frac{1}{2}\langle \underset{\sim}{S}_q\cdot\underset{\sim}{S}_{\bar{q}}\rangle\right)L^{ssM^2}(m_qR)\left(\frac{1}{2E_s-\omega_{TM}}+\frac{1}{2E_s+\omega_{TM}}\right)$$

$$+\frac{\delta^{IO}}{2}\left(\frac{3}{8}+\frac{1}{2}\langle \underset{\sim}{S}_q\cdot\underset{\sim}{S}_{\bar{q}}\rangle\right)C'^{ss}(m_qR,\ m_qR)$$

where δ^{IO} means that the term only contributes to the flavor singlet component, and E_s, is the mode energy of the radially excited s quark. ΔE_A is the contribution of diagrams (a)-(e) and (1), ΔE_B that of the remaining diagrams, (f)-(k).

Numerically the most important part of the $O(\alpha_s)$ energy shift is from diagrams (c), (d), (e) and (1). The spin splitting is dominated by diagram (c) and is therefore "normal", i.e. the higher spin states are more massive. Before discussing the "unusual" diagrams (f)-(k) we exhibit in Table 5 the meikton spectrum resulting from diagrams (a)-(e) and the self energies (1). We show only the $\alpha_s = 2.2$ fit (fit I)

as the variation between fits is fairly small--the overall scale varies by less than 100 MeV and the relative masses of the states by much less.

The predicted ordering of the states is 0^{-+}, 1^{-+}, 1^{--}, 2^{-+}. The meiktons are not as sensitive to C_{TE}/C_{TM} as the ground state glueballs (see Sec. 4) but do shift by about ±200 MeV as the ratio changes from 1/2 to 2. However their relative positions change by at most 20 MeV. The increase in mass for each extra strange quark or antiquark varies between 150 and 210 MeV--somewhat larger than the analogous spacing for the baryons.

We show in Table 6 the contribution of each diagram to the energy of the ω-like state with $C_{TE}/C_{TM} = 1$. These contributions can be obtained from the formulae for the energy of the meiktons ((5.1)-(5.4)) and Table 1. The table also includes the energy shift due to diagrams (f)-(k), the effects of which we now consider.

The sum of the Z-graphs, (h) and (i), has only a very small effect on the mass of the meiktons--20 MeV or less as Table 6 shows. However the small component of the meikton wavefunction, due to the Z and quark loop graphs, which consists of $\bar{q}\bar{q}qq$ may be very important in understanding the decays. As discussed in Sec. 6, if the meikton mass is above the appropriate threshold, the $\bar{q}\bar{q}qq$ state can "fall apart" into two mesons. Of theoretical interest, the factor 7/8 in the Z-graph contribution (see Eq. (5.4)) is a consequence of Fermi statistics.*

The s-channel Coulomb graph, (k), has a greater effect on the meikton masses. It effects the "ω" and the "φ" (using the vector nonet for the ideal mixing notation) in the $(0, 1, 2)^{-+}$ nonets, with

*see previous footnote.

the contribution to the "ω" being enhanced by a factor of 2 because this diagram can mix $\bar{u}u$ with $\bar{d}d$. The mass of the "ω" is raised relative to that of the "ρ" by about 100 MeV; the effect on the "φ" is only ~ 25 MeV because there is no factor of 2 and the Coulomb integral is half as large (see Table 1). There is also mixing between the "ω" and "φ" which effects the energy at $O(\alpha_s^2)$, beyond the order of our calculation. We have also checked that the $O(\alpha_s)$ "ω"-"φ" mixing is small, typically with mixing angle $|\theta| \lesssim 10°$.

The remaining diagrams, (f), (g) and (j), all give very small contributions to the meikton masses. However they all may be enhanced by perturbation theory "resonances". This corresponds to possibly substantial mixing with the particles in the intermediate states of these graphs--the d wave mesons, radially excited s-wave mesons and TE-TM glueballs for diagrams (f), (g) and (j) respectively.

A perturbation theory "resonance" occurs when an energy denominator in perturbation theory (Eq. (2.9)) vanishes. For example in diagram (j) the intermediate state TM gluon has a mode energy of 4.49/R, as compared to 4.08/R for the initial quark-antiquark pair. As the mass of the pair increases its mode energy increases and for mR ≅ .4 becomes equal to that of the TM gluon. Similar resonances occur in diagrams (f) and (g).

Close to a resonance the perturbative Eq. (2.9) is not valid. Instead the Hamiltonian must be diagonalised in the nearly degenerate basis of the meikton and the particle in the intermediate state. Because the final eigenvalues depend sensitively on the splitting of the diagonal elements of this mixing matrix, these must include all $O(\alpha_s)$ corrections except those responsible for the mixing. Thus the

effect of the mixing is very sensitive to the uncertainties in the bag model calculation, and in particular to the ratio C_{TE}/C_{TM}.

We can, however, make an estimate of the maximum magnitude of the shift due to the mixing: this shift is bounded by the off-diagonal element of the mixing matrix which we can calculate in the bag model. For diagram (f)--mixing with 1^{--} and 2^{-+} d-wave mesons--this matrix element is less than 20 MeV. For diagram (g)--mixing with 0^{-+} and 1^{--} radially excited s-wave mesons--the matrix element is about 50 MeV. Finally, diagram (j), which mixes the isoscalar members of the 0^{-+} and 2^{-+} nonets with glueballs, has a mixing matrix element of ~ 20 MeV for the "ω" and ~ 70 MeV for the "φ" of these nonets. Thus we do not expect this mixing to alter the general pattern of the states. This is particularly true of the 1^{-+} meiktons because the meson and glueball intermediate states for these meiktons are "spurious" states which we expect, as discussed above, to be heavier than their fixed cavity masses or to be absent. In either case the effect of mixing will be small.

In summary we predict four nonets of meiktons lying between 1.2 and 2.5 GeV. The predicted masses in Table 5 are considerably higher (400-800 MeV) than those obtained* in Ref. 10 because we have included all $O(\alpha_s)$ effects, in particular the quark and gluon self energies. We are in satisfactory agreement with Ref. 10 on the splitting between the states. The detailed structure of the nonets depends on the proximity of glueballs and radially and orbitally excited mesons. The most reliable prediction is for the exotic 1^{-+} nonet which may have no nearby states with which it can mix.

*We are comparing to the masses that follow from the formulae of Ref. 10 and not to the numerical values quoted there, which are augmented in Ref. 10 by ~ 200 MeV.

6. Phenomenology

In this section we discuss meikton phenomenology: how meiktons are produced and decay and how we may hope to identify them.*

Meikton production should be enhanced in processes which contain hard gluons in the final state. Gluon jets provide the clearest example. The gluon which forms the jet hadronizes by combining with either a color octet $\bar{q}q$ pair or with another gluon, which materialize from the color-confining QCD vacuum. The resulting hadron is respectively a meikton or a glueball,** just as the leading resonance in an s-quark jet should be a strange hadron. In theory gluon jets provide the best signal-to-noise for meikton production, but the practical problems of detection and reconstruction are severe.

Radiative ψ decay has a less favorable signal-to-noise ratio (the "noise" being from glueballs!). In perturbation theory meikton production in $\psi \to \gamma X$ is enhanced by α_s relative to ordinary mesons and suppressed by α_s relative to glueballs. The isoscalar members of the $(0, 1, 2)^{-+}$ nonets may all be produced in $\psi \to \gamma X$ in p-waves. In practice $\psi \to \gamma X$ is among the best places to search for meiktons.

Among hadronic experiments, the strong signal in $\bar{p}p$ annihilation at rest[41] attributed[38] to the glueball candidate i(1440) suggests this may also be a good source of meiktons. In particular, $(\bar{p}p)_{rest} \to X\pi\pi$ may be an excellent channel for the 0^{-+} and 1^{--} meiktons (if their masses are low enough) since in the $\bar{p}p$ s-wave, only for $J^{PC}(X) = 0^{-+}, 1^{--}$ can the $X\pi\pi$ final state be pure s-wave.

Other fixed target hadronic experiments will also be important.

*See also Ref. 10.

**For glueballs this mechanism was discussed in Ref. 40.

The study of meson spectroscopy in such experiments is essential, since disentangling the 1^{--}, 0^{-+}, and 2^{-+} meiktons from their $\bar{q}q$ meson counterparts requires a detailed understanding of the $\bar{q}q$ spectrum. This is especially true in those cases in which the meikton and $\bar{q}q$ mesons are significantly mixed. In fact we suggest below that the first evidence for a meikton may have been found in a high statistics pion scattering experiment in the $J^{PC} = 2^{-+}$ $f\pi$ final state.[27] This possibility illustrates a sense in which mixing is helpful: two states which are mixtures of a meikton and a $\bar{q}q$ meson can both be produced in typical hadronic experiments because of their $\bar{q}q$ components even if those experiments would not produce pure $\bar{q}qg$ states at a large rate. The likelihood that at least some meiktons will be substantially mixed with $\bar{q}q$ mesons therefore guarantees that fixed target hadronic experiments are a good way to search for meiktons.

How do meiktons decay? The lowest order diagram is shown in Fig. 5: the gluon creates a $\bar{q}q$ pair in the lowest available modes. The quark or antiquark formed by the gluon is in the $p_{1/2}$ or $p_{3/2}$ mode and the other is in the $s_{1/2}$ mode. The resulting four quark state, denoted schematically as $\bar{q}_s q_s(\bar{q}_s q_p + \bar{q}_p q_s)$, can "fall apart" in zeroeth order into two mesons, one in the s-wave ground state ($J^{PC} = 0^{-+}, 1^{--}$) and the other in the $L = 1$ excited state $(J^{PC} = (0, 1, 2)^{++}, 1^{+-})$. For example, the $I = 1$ member of the exotic $J^{PC} = 1^{-+}$ meikton nonet can decay in this way into πD or ηA_1.

We also encounter here, in another form, the issue of the "extra" or "spurious" bag model states discussed in Sec. 2. When $\bar{q}_s q_s(\bar{q}_s q_p + \bar{q}_p q_s)$ is organized into two color singlet $\bar{q}q$ pairs, in addition to the "normal" $L = 1$ states we also encounter the "extra" ones which are C-parity partners of the usual p-wave nonets, i.e., $J^{PC} = (0, 1, 2)^{+-}, 1^{++}$.

If the rigid cavity hypothesis were correct, these states would be nearly degenerate with their "normal" partners, $J^{PC} = (0, 1, 2)^{++}$, 1^{+-}, and would be produced in meikton decays recoiling against L = 0 mesons. It is clear however that if these "extra" states do exist, it is at a higher mass than the "normal" ones. They may then be too heavy to appear in meikton decays. If the extra states are truly spurious, i.e., at infinite mass, then the meikton decays involving them might be reinterpreted as p-wave decays of two s-wave mesons: for instance, the I = 1, $J^{PC} = 1^{-+}$ meikton may decay to $\pi\eta$. For intermediate values of the masses of the extra states (corresponding to intermediate values of the vacuum response time--see Sec. 2 and Ref. 12) there could be a significant amplitude for these "extra" $\bar{q}_s q_s(\bar{q}_p q_s + \bar{q}_s q_p)$ configurations to materialize as two L = 0 mesons in a relative p-wave. In discussing the meikton decay modes we will assume that these decays do occur. In any case they are certainly present in higher orders in cavity perturbation theory.

We now discuss the four meikton nonets in order of increasing ease of identification. The vector meikton nonet could be the most difficult to identify as meiktons. They cannot be produced in $\psi \to \gamma X$ and there are <u>two</u> $\bar{q}q$ nonets in the relevant mass region with which they can be confused and entangled: the radial excitation of the L = 0 nonet and the L = 2 vector meson nonet. It is not surprising that the experimental status of the vector mesons between $1\frac{1}{2}$ and 2 GeV is so unclear.[12,42] Some decays of the vector meiktons are

$$1^{--}\ \begin{cases} \text{"}\rho\text{"} \to \pi A_1,\ \rho\varepsilon,\ \pi^+\pi^-,\ \underline{K^S K^L},\ \underline{K^+K^-},\ \pi\eta \\ \qquad \pi\omega,\ \eta\rho,\ \underline{K\bar{K}^*},\ \rho^+\rho^- \\ \text{"}\omega\text{"} \to \pi B,\ \eta D,\ \underline{KQ}_{1,2},\ K^S K^L,\ K^+K^-,\ \pi\rho \\ \qquad \eta\omega,\ \underline{K\bar{K}^*},\ \rho\omega \\ \text{"}\phi\text{"} \to \underline{\eta E},\ KQ_{1,2},\ K^S K^L,\ K^+K^-,\ \eta\eta' \\ \qquad K\bar{K}^*,\ \underline{\eta\phi},\ \bar{K}^*K^* \\ \text{"}K^*\text{"} \to K + (A_1, D, \underline{E}, B),\ \pi Q_{1,2},\ K^*\varepsilon,\ \omega\kappa,\ \pi K \\ \qquad \pi K^*,\ \rho K,\ \underline{K\phi},\ \rho K^* \end{cases} \tag{6.1}$$

The underlined final states represent a possible way to distinguish meiktons from $\bar{q}q$ mesons of the same quantum numbers. These final states can occur in meiktons because in cavity perturbation theory the valence gluon can form an $\bar{s}s$ pair as readily as a $\bar{u}u + \bar{d}d$ pair (see Table 1). For $\bar{q}q$ mesons these decays are suppressed by the OIZ rule and by the suppression of $\bar{s}s$ creation from the QCD vacuum. For instance "ρ" $\to K\bar{K}$ would be OIZ allowed for a $\bar{q}q$ meson but is in fact suppressed in A_2 and f decays, presumably for the same reason that the K/π ratio is suppressed in the central region of hadron scattering. Similarly "K^*" $\to K\phi$ would be suppressed for a $s\bar{u}$ or $s\bar{d}$ meson because of both the OIZ rule and the suppression of $\bar{s}s$ creation in OIZ allowed configurations. Consequently, strong signals for the underlined decays would be characteristic of meikton production, particularly in the $I = \frac{1}{2}$, 1 channels in which glueballs cannot appear.

The 0^{-+} meikton nonet could be almost as difficult as the 1^{--} nonet to identify. For $C_{TE}/C_{TM} = \frac{1}{2}$ they lie in the region commonly attri-

buted to the radially excited $\bar{q}q$ 0^{-+} nonet, for which candidates exist for 8/9 of the nonet: $\pi'(1270)$, $K'(1400)$, and $\zeta(1275)$.[12] Among the expected decay modes are*

$$0^{-+} \begin{cases} \text{"}\rho\text{"} \to \pi\varepsilon,\ \eta\delta',\ \pi\rho,\ \omega\rho,\ \underline{KK^*},\ \underline{\kappa K} \\ \text{"}\omega\text{"} \to \eta\varepsilon,\ \pi\delta',\ \underline{KK^*},\ \underline{\kappa K} \\ \text{"}\phi\text{"} \to K\kappa,\ KK^*,\ \underline{\eta\phi} \\ \text{"}K^*\text{"} \to \pi\kappa,\ K\varepsilon,\ K\delta',\ K+(\rho,\ \omega,\ \underline{\phi}),\ \pi K^* \end{cases} \tag{6.2}$$

The best hope for identifying these states rests in finding more pseudoscalar states than can be accounted for as radial excitations of $\bar{q}q$ and in the characteristically meiktonic underlined decay modes.

For $C_{TE}/C_{TM} = 1/2$ the 2^{-+} meiktons also fall near observed states, in this case the nonet of the $A_3(1670)$, commonly presumed to be a d-wave $\bar{q}q$ state. A second $I = 1$ $J^{PC} = 2^{-+}$ state near the A_3 would be evidence for the existence of meiktons. In fact there is a peak in the $J^{PC} = 2^{-+}$ $f\pi$ channel at 1850 MeV,[27] far too low to be a radial excitation of A_3. This structure is best seen in the $f\pi$ d-wave, is perhaps also seen in $\varepsilon\pi$ and $\rho\pi$, but is not seen at all in the $f\pi$ s-wave which is the channel in which $A_3(1670)$ appears. This is what we would expect if a nearby meikton and meson were to mix strongly and the mixing were dominated by the $f\pi$ s-wave channel: one of the resulting eigenstates would then decouple from the $f\pi$ s-wave. The authors of Ref. 27 observe that their data could be explained by a new resonance

*δ' denotes the I, $J^{PC} = 1,\ 0^{++}$ $\bar{q}q$ state; we assume $\delta(980)$ is a $\bar{q}\bar{q}qq$ state.[1,12]

at 1850 MeV or perhaps at a higher mass. In a fit to four channels they find the A_3 at 1700 ±15 MeV and the second resonance at 2000 ±100 MeV. In this model the peak at 1850 in the $f\pi$ d-wave is the result of constructive interference between the A_3 and the state at 2000. Even in this case the 300 ±100 MeV splitting is rather small for the new state to be a radial excitation.

Decay modes of the 2^{-+} meikton nonet include the following:

$$2^{-+} \begin{cases} \text{"}\rho\text{"} \to \pi f,\ \eta A_2,\ \underline{KK^{**}},\ \pi\rho,\ \underline{KK^*},\ \rho\omega \\ \text{"}\omega\text{"} \to \eta f,\ \pi A_2,\ \underline{KK^{**}},\ \underline{KK^*} \\ \text{"}\phi\text{"} \to KK^{**},\ \underline{\eta f'},\ KK^* \\ \text{"}K^*\text{"} \to \pi K^{**},\ Kf,\ \underline{Kf'},\ KA_2,\ \pi K^*,\ K(\rho,\ \omega,\ \underline{\phi}) \end{cases} \tag{6.3}$$

To pursue the hint that the region from 1670 MeV to 1850 or 2000 MeV may contain a mixture of $I = 1$ $\bar{q}q$ and $\bar{q}qg$ states, it would be especially interesting to study the p-wave KK^* channel in this region.

The $J^{PC} = 1^{-+}$ channel is the cleanest in which to search for meiktons since we expect any glueballs and "extra" or "spurious" $\bar{q}q$ states with these quantum numbers to be at higher masses. As observed in Sec. 5, our predictions for the masses are also most reliable in this channel because of the expected absence of any nearby resonances. Some of the expected decays are

$$1^{-+}\left\{\begin{array}{l} \text{"}\rho\text{"} \to \pi D,\ \pi B,\ \eta A_1,\ \underline{\underline{\pi\eta}},\ \underline{\underline{\pi\eta'}},\ \eta\rho,\ \omega\rho,\ \underline{K\bar{K}^*},\ \underline{KQ}_{1,2} \\ \text{"}\omega\text{"} \to \pi A_1,\ \eta D,\ \eta B,\ \omega\varepsilon,\ KQ_{1,2},\ \underline{\underline{\eta\eta'}},\ \underline{K\bar{K}^*} \\ \text{"}\phi\text{"} \to KQ_{1,2},\ \underline{\eta E},\ \underline{\eta' E},\ \underline{\underline{\eta\eta'}},\ K\bar{K}^* \\ \text{"}K^*\text{"} \to KA_1,\ KB,\ \pi Q_{1,2},\ K^*\varepsilon,\ \underline{KE},\ KD,\ \pi K,\ \eta K \\ \qquad\quad \omega K,\ \rho K,\ \pi K^*,\ \eta K^*,\ \underline{K\phi},\ K^* + (\rho,\ \omega,\ \phi) \end{array}\right. \tag{6.4}$$

The decays "ρ" $\to \pi\eta$, $\pi\eta'$; "ω" $\to \eta\eta'$; and "ϕ" $\to \eta\eta'$ are double-underlined because in the p-wave they uniquely signal the 1^{-+} initial state ("ϕ" $\to \eta\eta'$ also merits a single underline because it signals the extra $\bar{s}s$ pair from the valence gluon). The decay "K^*" $\to \pi K$ (which occurs also for the 1^{--} meikton) is also noteworthy, since it is the only genuine two body decay mode among all the reactions we have considered.

To summarize this section, meiktons decay into two meson final states. They certainly decay to an $L = 0$ meson ($J^{PC} = 0^{-+}, 1^{--}$) and an $L = 1$ meson $\left(J^{PC} = (0, 1, 2)^{++}, 1^{+-}\right)$ in a relative s-wave and they might also decay to two $L = 0$ mesons in a relative p-wave. Because the TE valence gluon has an unsuppressed amplitude to create an $\bar{s}s$ pair some of the decays have a flavor structure which is not expected in the decays of $\bar{q}q$ mesons with the same quantum numbers, e.g., the $KK\bar{K}$ final state in "K^*" $\to \phi K$ or the decay "ρ" $\to K\bar{K}^*$. The 1^{--}, 0^{-+}, and 2^{-+} channels have the difficulty that meiktons must be distinguished from $\bar{q}q$ nonets of the same quantum numbers. But the data in the $I = 1$ $J^{PC} = 2^{-+}$ channel suggests this may not be an insuperable obstacle: if for instance the possible resonance at 1850 were confirmed and if both it and $A_3(1670)$ were observed to decay prominently to $K\bar{K}^*$, it

would constitute strong evidence for the hypothesis that the two states are mixtures of a meikton with the $\bar{q}q$ d-wave state. The exotic 1^{-+} channel is also a very promising hunting ground for the meiktons, especially in the p-wave $\pi\eta$, $\pi\eta'$, and $\eta\eta'$ final states. It would be interesting to look for the $\eta\eta'$ final state in radiative ψ decay.

7. Conclusion

If, as we expect, valence gluons exist, then meiktons must also exist. Even with only $\bar{q}q$ mesons the 1-2 GeV region is very densely populated, containing perhaps of the order of 15 nonets! The possible existence of glueballs in flavor singlets and meiktons in flavor nonets complicate an already highly complex particle spectrum, though it also greatly increases what we can learn.

We have used cavity perturbation theory to compute the meson, baryon, glueball and meikton spectrum. It is an open question whether this technique is merely a semiquantitative guide to the static properties of hadrons or whether it can be a truly quantitative approximation. The latter possibility is not excluded by the large value of α_s which the fits require, since the real expansion parameter is α_s times wave function overlap integrals, which is typically small.

Our main point is that incorporation of self energy effects is needed not only for theoretical consistency but may be phenomenologically very important. We have determined the self energy of the s-wave quark mode and of the sum of the TE and TM gluon modes by fitting to the s-wave meson and baryon spectrum and to the $J^{PC} = 0^{-+}$ glueball candidate at 1440 MeV. The quark self energy significantly improves the quality of the fit to the baryons and their static properties. The gluon self energy, which we find to be several times larger than that of the quark, has a big effect on our predictions of glueball and meikton masses. We expect the 2^{-+} glueball at ~ 2.3 GeV, of which more than 1 GeV is contributed by the self energy. For $C_{TE}/C_{TM} \geq 1/2$ our predictions for the meikton mass scale is raised by $\gtrsim 400$ MeV relative to what we would obtain with no self energies.

To show that cavity perturbation theory is a serious quantitative

approximation it is essential to calculate the self energies and compare the result with experiment. Machinery which could be applied to this calculation has been developed.[35] It would be very interesting to know whether the calculated self energies agree with our fits and whether the $O(\alpha_s^2)$ contributions are indeed smaller than the $O(\alpha_s)$ terms. The question of convergence is of particular interest for the gluon self energy which our fit requires to be especially large.

The experimental side of this program is to find the states with valence gluons. The interpretation of i(1440) needs clarification: an important step would be the discovery of a tenth pseudoscalar which could fill the π' nonet leaving an odd man out. More glueballs are needed to determine the unknown ratio C_{TE}/C_{TM}.

A good meikton candidate could also fix this ratio by determining C_{TE}. If the A_3 and the possible resonance above it are a mixture of a meikton with a d-wave $\bar{q}q$ meson, then it appears from Table 4 that C_{TE}/C_{TM} is between 1/2 and 1. More data on this region would be very interesting, especially in the KK^* channel that would uniquely characterize an isovector meikton. Similarly it would be useful to study three kaon channels, such as $K\phi$ and KE, which uniquely characterize the strange meiktons. The exotic 1^{-+} channel is excellent for the search for meiktons, having clean two body decay modes such as $\pi\eta$, $\eta\eta'$, and πK.

To find the meiktons and glueballs the program in meson spectroscopy must be pursued with great vigor. Partial wave analyses must be extended upward in mass and statistics, in radiative ψ decay and in fixed target hadron experiments.

Acknowledgments

We wish to thank T. Barnes, F. Close, and T. DeGrand for helpful discussions and correspondence.

This work was supported by the Director, Office of Energy Research, Office of High Energy and Nuclear Physics, Division of High Energy Physics of the U.S. Department of Energy under contract DE-AC03-76SF00098.

Appendix 1

In this appendix we give the formulae for the vertices in Table 1 and compare our notation to that of other authors. Throughout this appendix we set $R = 1$.

The L-wave ($L = 0, 1 \ldots$) quark modes in a spherical cavity are:

$$N_{\ell,\varepsilon} \begin{pmatrix} j_\ell(kr)\ U_{j,\ell,m}(\Omega) \\ -i\,\frac{k}{E+m}\,\varepsilon\, j_{\ell+\varepsilon}(kr)\ U_{j,\ell+\varepsilon,m}(\Omega) \end{pmatrix} \tag{A1.1}$$

where $j = \ell + \frac{\varepsilon}{2}$ and $\varepsilon = \pm 1$, and the spinor spherical harmonics are defined by:

$$U_{j,\ell,m}(\Omega) = \sum_{\mu} Y_{\ell\mu}(\Omega)\ u_{m-\mu} < \ell,\mu;\, 1/2\ ,\ m-\mu \,|\, j,\mu > \tag{A1.2}$$

where u is a Pauli spinor. The values of k are determined by

$$\frac{\varepsilon k}{E+m}\, j_{\ell+\varepsilon}(k) = j_\ell(k) \tag{A1.3}$$

and the normalization is given by:

$$N_{\ell,\varepsilon} = \frac{k}{j_\ell(k)\left[2E\left(E - \varepsilon(\ell+1)\right) + m\right]^{1/2}} \ . \tag{A1.4}$$

The general expressions for TE and TM gluon modes in Coulomb gauge are given in Ref. 3. However, to make the expressions for the vertices as simple as possible, we prefer to consider the general cavity eigenstates without the Coulomb gauge condition. These are:

$$\underset{\sim}{A}_{j,\ell,m}(\underset{\sim}{r}) = \alpha_{j,\ell}\, j_\ell(\omega r)\ \underset{\sim}{Y}_{j,\ell,m}(\Omega) \tag{A1.5}$$

where $L = j+1,\ j,\ j-1$, the $\underset{\sim}{Y}$ are vector spherical harmonics (e.g. see Ref. 3), and the normalization constants are defined by:[3]

$$\alpha_{j,j} = \frac{1}{j_j(\omega)\left[\omega\left(1-\frac{j(j+1)}{\omega}\right)\right]^{1/2}} \tag{A1.6}$$

$$\alpha_{j,j\pm1} = \frac{1}{j_{j+1}(\omega)\omega^{1/2}}$$

For $L = j$ ω satisfies TE boundary conditions and for $L = j \pm 1$ TM boundary conditions as given in Ref. 3. The connection to TE and TM modes is:

$$\underset{\sim}{A}^{TE}_{j,m}(\underset{\sim}{r}) = \underset{\sim}{A}_{j,j,m}(\underset{\sim}{r}) \tag{A1.7}$$

$$\underset{\sim}{A}^{TM}_{j,m}(\underset{\sim}{r}) = \sqrt{\frac{j+1}{2j+1}}\ \underset{\sim}{A}_{j,j-1,m}(\underset{\sim}{r}) - \sqrt{\frac{j}{2j+1}}\ \underset{\sim}{A}_{j,j+1,m}(\underset{\sim}{r}) \quad .$$

Now consider the vertex

$$\text{quark}_i(j_1,\varepsilon_1,m_1) \to \text{quark}_j(j_2,\varepsilon_2,m_2) + \text{"gluon}_a\text{"}(j_3,\ell_3 m_3)$$

where i, j and a are color indices. Extracting a factor

$$\sqrt{\alpha_s}\ \ T^a_{ji}\ \ i\langle j_2,m_2;j_3,m_3|j_1,m_1\rangle$$

leaves the L factor

$$L^{(j_1\varepsilon_1)(j_2\varepsilon_2)(j_3\ell_3)} = \left(6(2j_2+1)(2j_3+1)\right)^{1/2} N_{\ell_1,\varepsilon_1} N_{\ell_2,\varepsilon_2} \alpha_{j_3,\ell_3} \tag{A1.8}$$

$$\left[-\varepsilon_1\left(\frac{k_1}{E_1+m_1}\right)\left((2\ell_2+1)(2\ell_3+1)\right)^{1/2}\langle \ell_2,0;\ell_3,0|\ell_1+\varepsilon_1,0\rangle \right.$$

$$\times \begin{Bmatrix} \ell_2 & \ell_3 & \ell_1+\varepsilon_1 \\ 1/2 & 1 & 1/2 \\ j_2 & j_3 & j_1 \end{Bmatrix} \int_0^1 r^2 dr\ j_{\ell_2}(k_2 r) j_{\ell_3}(\omega_3 r) j_{\ell_1+\varepsilon_1}(k_1 r)$$

$$+\varepsilon_2\left(\frac{k_2}{E_2+m_2}\right)\left((2(\ell_2+\varepsilon_2)+1)(2\ell_3+1)\right)^{1/2}\langle \ell_2+\varepsilon_2,0;\ell_3,0|\ell_1,0\rangle$$

$$\left. \times \begin{Bmatrix} \ell_2+\varepsilon_2 & \ell_3 & \ell_1 \\ 1/2 & 1 & 1/2 \\ j_2 & j_3 & j_1 \end{Bmatrix} \int_0^1 r^2 dr\ j_{\ell_2+\varepsilon_2}(k_2 r) j_{\ell_3}(\omega_3 r) j_{\ell_1}(k_1 r) \right]$$

where the Wigner 9j symbol has been used. The TE and TM vertices can be obtained using Eq. (A1.7). The parity selection rules are contained in the Clebsch-Gordon coefficients in Eq. (A1.8). We have left the radial integrals because we have found it simplest to do them numerically. The antiquark vertex is identical except that $T^a_{ji} \to -T^a_{ij}$. Finally, to obtain some of the results in Table 1 we need

$$\langle 1/2,m_1;1,m_3|1/2,m_2\rangle = \sqrt{\frac{4}{3}}\ \underset{\sim}{S}_{m_1 m_2}\cdot\underset{\sim}{e}^*_{m_3} \quad . \tag{A1.9}$$

Next we consider the vertex of general form

$$\text{quark}_i(j_1,\varepsilon_1,m_1) + \text{antiquark}_j(j_2,\varepsilon_2,m_2) \to \text{"gluon}_a\text{"}(j_3,\ell_3,m_3).$$

Extracting the factor

$$\sqrt{\alpha_s}\, T^a_{ji} \langle j_1,m_1;j_2,m_2\ j_3,m_3\rangle$$

leaves:

$$L^{(j_1\varepsilon_1)(j_2\varepsilon_2)(j_3\ell_3)} = \left(6(2j_1+1)(2j_2+1)\right)^{1/2} \acute{N}_{\ell_1,\varepsilon_1} N_{\ell_2,\varepsilon_2}{}^{\alpha}{}_{j_3,\ell_3} \tag{A1.10}$$

$$\left[\left((2\ell_1+1)(2\ell_2+1)\right)^{1/2} \langle \ell_1,0;\ell_2,0|\ell_3,0\rangle \right.$$

$$\times \begin{Bmatrix} \ell_1 & \ell_2 & \ell_3 \\ 1/2 & 1/2 & 1 \\ j_1 & j_2 & j_3 \end{Bmatrix} \int_0^1 r^2 dr\ j_{\ell_1}(k_1 r) j_{\ell_2}(k_2 r) j_{\ell_3}(\omega_3 r)$$

$$+ \varepsilon_1\varepsilon_2 \left(\frac{k_1}{E_1+m_1}\right)\left(\frac{k_2}{E_2+m_2}\right) \left[\left(2(\ell_1+\varepsilon_1)+1\right)\left(2(\ell_2+\varepsilon_2)+1\right)\right]^{1/2}$$

$$\times \langle \ell_1+\varepsilon_1,0;\ell_2+\varepsilon_2,0|\ell_3,0\rangle$$

$$\left. \times \begin{Bmatrix} \ell_1+\varepsilon_1 & \ell_2+\varepsilon_2 & \ell_3+\varepsilon_3 \\ 1/2 & 1/2 & 1 \\ j_1 & j_2 & j_3 \end{Bmatrix} \int_0^1 r^2 dr\ j_{\ell_1+\varepsilon_1}(k_1 r) j_{\ell_2+\varepsilon_2}(k_2 r) j_{\ell_3}(\omega_3 r) \right] .$$

There is no ambiguity between the notation for L factors in Eqs. (A1.8) and (A1.10) because of the parity selection rules. To obtain the results of Table 1 we also need

$$\langle 1/2,m_1;1/2,m_2|1,m_3\rangle = \sqrt{2}\, \underset{\sim}{S}_{-m_2,m_1} \cdot \underset{\sim}{e}^*_{m_3} \ . \tag{A1.11}$$

The relationship of our notation to that of other authors for the quark-gluon vertices is as follows.

Close and Horgan[20]: $$\left(\sqrt{4\pi}\ I\right) = \sqrt{\frac{\omega_{gluon}}{2}}\ L \tag{A1.12}$$

Close and Monaghan[34]: $$I = \sqrt{\frac{\omega_{gluon}}{2}}\ L \tag{A1.13}$$

Maciel and Monaghan[34] quote numerical coefficients for all the vertices shown in Table 1 for massless quarks. For the vertices involving only $j = 1/2$ quarks our L factors can be obtained from their coefficients by multiplying by a factor of $4\sqrt{\pi}$. For the other vertices, e.g. involving $p_{3/2}$ quarks, they use different spin tensors than us and the relative factors vary from vertex to vertex.

The $(TE)^3$ 3-gluon vertex is discussed in Ref. 3 in detail. The relationship between the t_1 of Ref. 3 and our L factor is

$$L^{TE\,TE\,TE} = \sqrt{\pi}\ t_1 \ . \tag{A1.14}$$

Also we use a g of opposite sign to that of Ref. 3 which, though it has no effect on the final results, effects some of the signs in Table 1.

This leaves the Coulomb graphs. We will not give general expressions as they are very cumbersome. The t-channel Coulomb vertices only involve the $L = 0$ part of the Coulomb propagator because the s-wave modes have a spherically symmetric charge density. Thus C^{ss} and C^{sTE} are given by (using Eqs. (2.3) and (2.5)):

$$C^{ab} = \int_0^1 r^2 dr\ \rho_a(r) \int_0^r r'^2 dr'\ \rho_b(r') \left(\frac{1}{r} - 1 \right) + a \leftrightarrow b \qquad \text{(A1.15)}$$

where the charge density of an s-quark or antiquark is:

$$\rho_s(r) = N_s^2 \left[j_0^2(k_s r) + \left(\frac{k_s}{E_s + m} \right)^2 j_1^2(k_s r) \right] \qquad \text{(A1.16)}$$

and the $\ell = 0$ projection of the charge density of a 1^{+-} TE gluon is

$$\rho_{TE}(r) = 2\ \alpha_{TE}^2 \omega_{TE}\ j_1^2(\omega_{TE} r) \quad . \qquad \text{(A1.17)}$$

We have used the notation of Eqs. (2.10)-(2.13).

Finally the s channel Coulomb vertex, to which only the L = 1 part of the Coulomb propagator contributes, is:

$$C'^{s_1 s_2} = \frac{2}{9} \int_0^1 r^2 dr\ \rho_{s_1}(r) \int_0^r r'^2 dr'\ \rho^*_{s_2}(r') \left(\frac{r'}{r^2} + 2rr' \right) + s_1 \leftrightarrow s_2 \qquad \text{(A1.18)}$$

with,

$$\rho_s(r) = 2\ N_s^2 \frac{ik_s}{E_s + m}\ j_0(k_s r) j_1(k_s r) \quad . \qquad \text{(A1.19)}$$

This vertex has also been calculated by Maciel and Monaghan.[34] Our C' factor is obtained by multiplying their coefficient by a factor of 16π.

Appendix 2

Here we show that the results of Ref. 3 (BCM) and Ref. 4 (CHP) for the energy shift of (TE)(TM) glueballs due to the 4-gluon vertex are compatible. We will use the notation of BCM for the operators in spin space, and also use their notation for the standard integrals, I_1, I_2 and I_3 (Eq. (3.23) of BCM).

BCM distinguish the direct contribution of the 4 gluon vertex

$$\Delta E_{BCM1} = - 6 \frac{\alpha_s}{R} \left(\frac{I_1}{3} \left\langle \underset{\sim}{S}^{EE} \cdot \underset{\sim}{S}^{MM} \right\rangle \right) \qquad \text{(A2.1)}$$

and the exchange contribution

$$\Delta E_{BCM2} = - 6 \frac{\alpha_s}{R} \left[\frac{4}{9} I_1 \left\langle \phi^{EM} \phi^{ME} \right\rangle + \frac{1}{6} (I_1 + 2I_2 + I_3) \left\langle \underset{\sim}{S}^{EM} \cdot \underset{\sim}{S}^{ME} \right\rangle + \left(\frac{1}{3} I_1 + \frac{2}{5} I_2 + \frac{1}{5} I_3 \right) \left\langle T^{EM} \cdot T^{ME} \right\rangle \right] \qquad \text{(A2.2)}$$

where Eqs. (3.18), (3.22), (3.23) and (3.24) of BCM have been used, and where $\underset{\sim}{S}^{EE}$ is the spin operator acting between the initial and final TE modes, etc.

The CHP result (E.18, E.19 of Ref. 4) can be written as

$$\Delta E_{CHP} = - 6 \frac{\alpha_s}{R} \left[\left(\frac{1}{15} (2I_2 + I_3) - \frac{1}{2} C_{EM}^{4g} \right) \left\langle \phi_1 \phi_2 \right\rangle + \frac{1}{6} (2I_1 + 2I_2 + I_3) \left\langle \underset{\sim}{S}_1 \cdot \underset{\sim}{S}_2 \right\rangle + \frac{1}{5} (2I_2 + I_3) \left\langle T_1 \cdot T_2 \right\rangle \right] \qquad \text{(A2.3)}$$

where the transformation:

$$T_{12} = 2T_1 \cdot T_2 + \frac{2}{3}\,\phi_1\phi_2 \qquad \text{(A2.4)}$$

from CHP's to BCM's spin operators has been used. C_{EM}^{4g} is CHP's spin independent coefficient which they do not display, and they do not state whether their spin operators are in the direct or the exchange basis or in some mixture of these bases.

Adding (A2.1) and (A2.2) to get the total result of BCM does not give the same coefficients of either of the spin independent terms as (A2.3). However after a Fierz transformation of Eq. (A2.1) to rewrite it in the exchange basis of (A2.2) we find (using BCM's Eq. (A2.7) for the Fierz transformation):

$$\Delta E_{BCM1} = -\,6\,\frac{\alpha_s}{R}\left[\frac{2I_1}{9}\left\langle \phi^{EM}\phi^{ME}\right\rangle + \frac{I_1}{6}\left\langle \underset{\sim}{S}^{EM}\cdot\underset{\sim}{S}^{ME}\right\rangle - \frac{I_1}{3}\left\langle T^{EM}\cdot T^{ME}\right\rangle\right] \qquad \text{(A2.5)}$$

When added to (A2.2) this now agrees with the coefficients of the spin dependent terms found by CHP, Eq. (A2.3). Then there is no disagreement as long as:

(i) CHP's operators are in the exchange basis; and

(ii) the coefficients of $\left\langle \phi_1\phi_2\right\rangle$ agree, i.e.

$$C_{4g}^{EM} = -\frac{4}{3}\,I_1 + \frac{2}{15}\,(2I_2+I_3) \quad . \qquad \text{(A2.6)}$$

References

1. R. Jaffe and K. Johnson, Phys. Lett. 60B (1976) 201.
2. J. Donoghue, K. Johnson, and B.A. Li, Phys. Lett. 99B (1981) 416.
3. T. Barnes, F. Close, and S. Monaghan, Nucl. Phys. B198 (1982) 380.
4. C. Carlson, T. Hansson, and C. Peterson, SLAC-PUB-2873 (1982).
5. T. Barnes, Z. Phys. C10 (1981) 275.
6. J.M. Cornwall and A. Soni, UCLA preprint (1982).
7. F. Close, RL-81-066 (1981 EPS Intl. Conference on High Energy Physics, Lisbon, July 1981).
8. P. Hasenfratz, R. Horgan, J. Kuti, and J.M. Richard, Phys. Lett. 95B (1980) 299.
9. F. deViron and J. Weyers, Nucl. Phys. B185 (1981) 391.
10. T. Barnes and F. Close, RL-82-037, 1982.
11. T. DeGrand and R. Jaffe, Ann. Phys. 100 (1976) 425.
12. M. Chanowitz, Proc. SLAC Summer Inst. (ed. A. Mosher) 1981.
13. A. DeRujula, H. Georgi, and S. Glashow, Phys. Rev. D12 (1975) 147.
14. G. 't Hooft, Nucl. Phys. B72 (1974) 461.
15. E. Witten, Nucl. Phys. B156 (1979) 269.
16. P. Lepage, Proc. SLAC Summer Inst. (ed. A. Mosher) 1981; C. Matteuzzi, Particles and Fields 1981 (AIP Conf. Proc. No. 81, eds. C. Heusch and W. Kirk) 186.
17. J. Kogut et al., Phys. Rev. Lett. 43 (1979) 484; M. Creutz, Phys. Rev. D21 (1980) 2308.
18. T. DeGrand et al., Phys. Rev. D12 (1975) 2060.
19. T.D. Lee, Phys. Rev. D19 (1979) 1802.
20. F. Close and R. Horgan, Nucl. Phys. B164 (1980) 413.
21. S. Mandelstam, Proc. Intl. Symp. on Lepton and Photon Interactions (FNAL) 1979.

22. C. Callan et al., Phys. Rev. D17 (1978) 2717.

23. M. Chanowitz, Particles and Fields 1981 (AIP Conf. Proc. No. 81, eds. C. Heusch and W. Kirk) 85.

24. M. Franklin et al., presented at the meeting of the A.P.S., Washington, D.C., April 1982; D. Burke, presented at the Intl. Conf. on Elementary Particle Physics, Paris, 1982.

25. M. Chanowitz, manuscript in preparation.

26. C. Peterson, T. Hansson, and K. Johnson, Phys. Rev. D26 (1982) 415.

27. C. Daum et al., Phys. Lett. 89B (1980) 285.

28. M. Chanowitz and S. Sharpe, manuscript in preparation.

29. C. Rebbi, Phys. Rev. D12 (1975) 2407 and D14 (1976) 2362.

30. T. DeGrand, Ann. Phys. 101 (1976) 496.

31. C. Bender and P. Hays, Phys. Rev. D14 (1976) 2262.

32. K. Milton, Phys. Rev. D22 (1980) 1441.

33. O. Maxwell and V. Vento, Saclay DPh-T/81-76 (1981).

34. F. Close and S. Monaghan, Phys. Rev. D23 (1981) 2098; A. Maciel and J. Paton, Nucl. Phys. B197 (1982) 201; A. Maciel and S. Monaghan, Oxford 25/82 (1982).

35. T. Hansson and R. Jaffe, manuscript in preparation.

36. J. Donoghue and K. Johnson, Phys. Rev. D21 (1980) 1975.

37. R. Konoplich and M. Schepkin, Nuovo Cim. 67A (1982) 211.

38. M. Chanowitz, Phys. Rev. Lett. 46 (1981) 981.

39. C. Thorne, unpublished (cited in Ref. 2).

40. J. Bjorken, Proc. SLAC Summer Inst. (ed. A. Mosher) 1979; P. Roy and T. Walsh, Phys. Lett. 78B (1979) 62.

41. P. Baillon et al, Nuovo Cim. A50 (1967) 393.

42. B. Kumar, Experimental Meson Spectroscopy—1980 (AIP Conf. Proc. No. 67, eds. S. Chung and S. Lindenbaum).

TABLE 1. Vertices needed at $O(\alpha_s)$ for the meson, baryon and meikton energies. Vertices with antiquarks can be obtained from those with quarks by making the substitutions: $\underset{\sim}{S} \to -\underset{\sim}{S}^T$ and $T^a \to -T^{a^T}$. The gluon spin matrix is $\underset{\sim}{S}_{m_c m_b} = i\,\underset{\sim}{e}_{m_b} \times \underset{\sim}{e}^*_{m_c}$. Indices i and f refer to both quark spin and color. s' means the first radially excited s quark. Dashed lines represent Coulomb Green functions. A Fierz transformation has been done on the spin factor of the s-channel Coulomb vertex.

VERTEX	FORM OF VERTEX	L or C Factor		
		mR = 0	mR = 2 1 quark	mR = 2 2 quarks
TE,b ~ TE,c / TE,a	$\frac{\sqrt{\alpha_s}}{R}\,\underset{\sim}{S}_{m_c m_b}\cdot\underset{\sim}{e}^*_{m_a}\left(-f^{acb}\,L^{EEE}\right)$	.340		
S,i → S,f / TE,a	$\frac{\sqrt{\alpha_s}}{R}\,\underset{\sim}{S}_{fi}\cdot\underset{\sim}{e}^*_{m_a}\,T^a_{fi}\left(-i\,L^{ssE}\right)$	.985	.714	
S,i → S',f / TE,a	$\frac{\sqrt{\alpha_s}}{R}\,\underset{\sim}{S}_{fi}\cdot\underset{\sim}{e}^*_{m_a}\,T^a_{fi}\left(-i\,L^{ss'E}\right)$	-.131	-.135	
S,i / S,i' ~ TM,a	$\frac{\sqrt{\alpha_s}}{R}\,\underset{\sim}{S}_{i'i}\cdot\underset{\sim}{e}^*_{m_a}\,T^a_{i'i}\,L^{SSM}$	-.120	-.583	
S,i / $P_{\frac{1}{2},i'}$ ~ TE,a	$\frac{\sqrt{\alpha_s}}{R}\,\underset{\sim}{S}_{i'i}\cdot\underset{\sim}{e}^*_{m_a}\,T^a_{i'i}\,L^{SPE}$	-.650	-.886	
S,i / $P_{\frac{1}{2},i'}$ ~ TE,a	$\frac{\sqrt{\alpha_s}}{R}\,\left\langle \frac{1}{2}\,m_i,\frac{3}{2}\,m_i',\middle\vert 1m_a\right\rangle\,T^a_{i'i}\,L^{SP'E}$	-.591	-.570	
$D_{\frac{3}{2},i}$ → S,f / TE,a	$\frac{\sqrt{\alpha_s}}{R}\,i\,\left\langle \frac{1}{2}\,m_f,1m_a\middle\vert \frac{3}{2}\,m_i\right\rangle\,T^a_{fi}\,L^{sdE}$	.020	.031	
S,i → S,f / S,i' → S,f'	$\frac{\alpha_s}{R}\,T^a_{fi}T^a_{f'i'}\,C^{ss}$	.278	.349	.448
S,i — S,f / TE,b ~ TE,c	$\frac{\alpha_s}{R}\,T^a_{fi}\left(-if^{acb}\,C^{SE}\right)$	.217	.261	
S,i ⤳ S,f / S,i' ⤳ S,f'	$\frac{\alpha_s}{R}\left(\frac{3}{8}\,\delta_{fi}\delta_{f'i'}+\frac{1}{2}\,\underset{\sim}{S}_{fi}\cdot\underset{\sim}{S}_{f'i'}\right)T^a_{i'i}T^a_{f'f}\,C^{'ss}$	.600	.417	.306

TABLE 2. Various fits to the mesons and baryons.

The parameters of the fits are:

fit I $B^{1/4} = .144$ GeV, $Z_0 = -2.45$, $m_s = .34$ GeV, $\alpha_s = 2.2$, $C_Q = .30$;

fit II $B^{1/4} = .120$ GeV, $Z_0 = -2.99$, $m_s = .34$ GeV, $\alpha_s = 2.8$, $C_Q = .48$;

MIT fit[18] $B^{1/4} = .145$ GeV, $Z_0 = -1.84$, $m_s = .279$ GeV, $\alpha_s = 2.2$. *

Masses are in units of GeV and radii in GeV^{-1}. The η_s is a hypothetical $\bar{s}s$ pseudoscalar meson. In the case of the MIT fit, the underlined particles were used to fix the parameters of the fit.

PARTICLE	EXPERIMENTAL MASS	FIT I MASS	FIT I RADIUS	FIT II MASS	FIT II RADIUS	MIT FIT MASS	MIT FIT RADIUS
N	0.939	0.959	5.15	0.955	6.50	<u>0.938</u>	5.00
Λ	1.116	1.127	5.07	1.125	6.37	<u>1.105</u>	4.95
Σ	1.193	1.175	5.08	1.185	6.39	1.144	4.95
Ξ	1.318	1.315	5.00	1.319	6.26	1.289	4.91
Δ	1.232	1.250	5.59	1.246	7.07	<u>1.233</u>	5.48
Σ^*	1.384	1.398	5.52	1.391	6.96	<u>1.382</u>	5.43
Ξ^*	1.533	1.541	5.45	1.530	6.85	1.529	5.39
Ω	1.672	1.681	5.38	1.664	6.74	<u>1.672</u>	5.35
ρ/ω	0.776	0.755	4.73	0.760	5.92	<u>0.783</u>	4.71
K^*	0.894	0.895	4.64	0.895	5.81	<u>0.928</u>	4.65
ϕ	1.019	1.027	4.56	1.019	5.74	1.068	4.61
π	0.138	0.245	3.22	0.251	4.15	0.280	3.34
K	0.496	0.469	3.07	0.493	3.91	0.497	3.26
η_s	--	0.670	3.02	0.699	3.85	--†	--†

*The MIT fit does not include the quark self energy as discussed in the text.

†The MIT fit did not quote an η_s mass.

TABLE 3. Baryon magnetic moments in units of nuclear magnetons. (a) The static bag model values. (b) The values after inclusion of the momentum spread of the wave packet using the model of Donoghue and Johnson.[36]

PARTICLE	EXPERIMENT	MIT FIT	FIT II	MIT FIT	FIT II
p	2.793	1.90	2.46	2.33	2.78
n	-1.913	-1.27	-1.64	-1.56	-1.85
Λ	-0.614 ± 0.005	-0.48	-0.54	-0.56	-0.59
Σ^+	2.32 ± 0.14	1.84	2.34	2.13	2.54
Σ^0		0.59	0.72	0.68	0.78
Σ^-	-0.89 ± 0.14	-0.68	-0.89	-0.79	-0.97
Ξ^0	-1.24 ± 0.16	-1.06	-1.23	-1.19	-1.32
Ξ^-	-0.70 ± 0.03	-0.44	-0.44	-0.49	-0.47

TABLE 4. Predictions of glueball masses with various assumptions for the self energies ratio C_{TE}/C_{TM} and for the two fits to the mesons and baryons discussed earlier. All masses are in GeV. and all radii in GeV.$^{-1}$. The 1.44 mass is an input parameter.

GLUEBALL			0^{++}		2^{++}		0^{-+}		2^{-+}	
FIT	C_{TE}/C_{TM}	C_{TE}	C_{TM}	MASS	RADIUS	MASS	RADIUS	MASS	RADIUS	MASS	RADIUS
I	1/2	1.19	2.37	0.67	4.54	1.75	6.25				
	1	1.78	1.78	1.14	5.42	2.12	6.66	1.44	5.86	2.30	6.8
	2	2.37	1.19	1.56	6.01	2.47	7.01				
II	1/2	1.82	3.64	0.65	5.70	1.74	7.93				
	1	2.73	2.73	1.21	7.04	2.18	8.55	1.44	7.45	2.30	8.7
	2	3.64	1.82	1.70	7.87	2.59	9.06				

TABLE 5. The meikton spectrum for our fit I and $C_{TE}/C_{TM} = 1/2, 1, 2$. Only diagrams (a)-(e) and the self energies (1) are included, and so all the nonets are ideally mixed. Thus we label them by analogy with the vector mesons. All masses are in GeV. and all radii in $GeV.^{-1}$.

J^{PC}	TYPE	$C_{TE}/C_{TM} = 1/2$		$C_{TE}/C_{TM} = 1$		$C_{TE}/C_{TM} = 2$	
		Mass	Radius	Mass	Radius	Mass	Radius
1^{--}	ρ/ω	1.64	6.10	1.83	6.35	2.02	6.56
	K^*	1.80	6.03	1.99	6.29	2.18	6.50
	ϕ	1.96	5.95	2.16	6.22	2.35	6.44
0^{-+}	ρ/ω	1.20	5.50	1.41	5.81	1.61	6.05
	K^*	1.41	5.42	1.62	5.74	1.82	5.98
	ϕ	1.61	5.34	1.82	5.67	2.03	5.91
1^{-+}	ρ/ω	1.41	5.80	1.61	6.05	1.80	6.31
	K^*	1.59	5.73	1.80	5.98	1.99	6.25
	ϕ	1.78	5.66	1.99	5.90	2.18	6.18
2^{-+}	/	1.79	6.30	1.97	6.51	2.15	6.70
	K^*	1.94	6.24	2.13	6.45	2.31	6.65
		2.09	6.17	2.28	6.39	2.47	6.59

TABLE 6. A breakdown of the energy of the ω-like meikton of all the nonets for $C_{TE}/C_{TM} = 1$ and fit I. All energies are in MeV.

	1^{--}	0^{-+}	1^{-+}	2^{-+}
Bag energy	461	353	399	497
Mode energy	1076	1175	1129	1049
"Zero point" energy	-386	-422	-405	-376
Diagram (a)	30	-11	-11	-10
" (b)	16	18	17	16
" (c)	0	-555	-266	248
" (d)	-226	-247	-237	-220
" (e)	92	257	171	20
" (l)	770	841	808	751
Total $O(\alpha_s)$	682	303	482	805
Total (See Table 4)	1833	1408	1605	1975
Diagram (f)	-1	0	0	-1
(g)	-7	-21	-14	0
(h)	7	40	23	-9
(i)	11	-20	-4	24
(j)	0	-6	-6	-5
(k)	0	114	109	101

Figure Captions

Figure 1: Self energy graphs for (a) quarks and (b) gluons. Only one time ordering of each graph is shown. The thick dashed line shows the intermediate state where appropriate and the thin dashed line represents the cavity Coulomb Green function.

Figure 2: Diagrams contributing at $O(\alpha_s)$ to the energy of the mesons and baryons. The notation is as in Figure 1. Only one time ordering is shown. The self energy graphs are represented as a blob and only the quark self energy is shown.

Figure 3: The $O(\alpha_s)$ diagrams contributing to glueball energies for (a) the 0^{++} and 2^{++} glueballs, and (b) for the 0^{-+} and 2^{-+} glueballs. Where not stated TE and TM refer to the modes with $J^{PC} = 1^{+-}$ and 1^{--} respectively. The notation is as in previous figures.

Figure 4: The $O(\alpha_s)$ diagrams contributing to the energies of the meiktons. The notation is the same as in previous figures. Diagrams obtained by interchanging quark and antiquark are not shown. The possible intermediate states are noted with each diagram ($s'_{1/2}$ is the first radial excitation of the $s_{1/2}$quark and TE and TM refer to the 1^{+-} and 1^{--} modes respectively); for diagrams with two labels the first (second) label corresponds to the first (second) noted intermediate state.

Figure 5: The diagrams corresponding to the dominant decay mechanism of the meiktons.

(a)

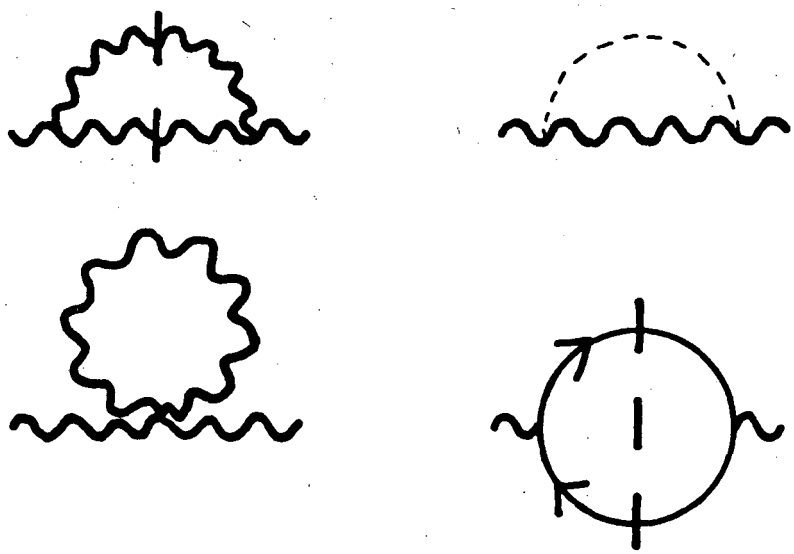

(b)

Figure 1

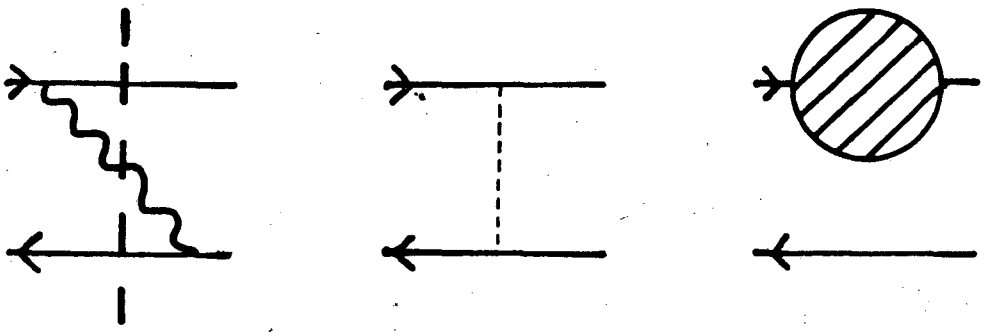

Figure 2

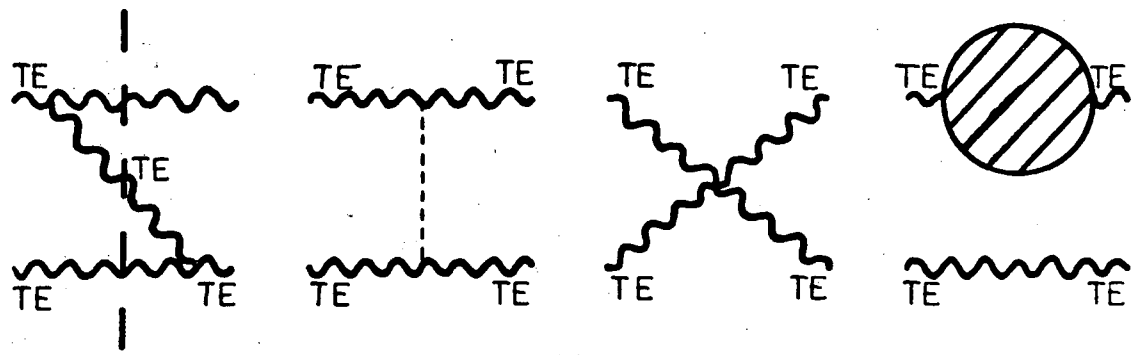
TE
TE
TE
TE
TE
TE
TE
TE
TE
TE
TE
TE
TE
TE

(a)

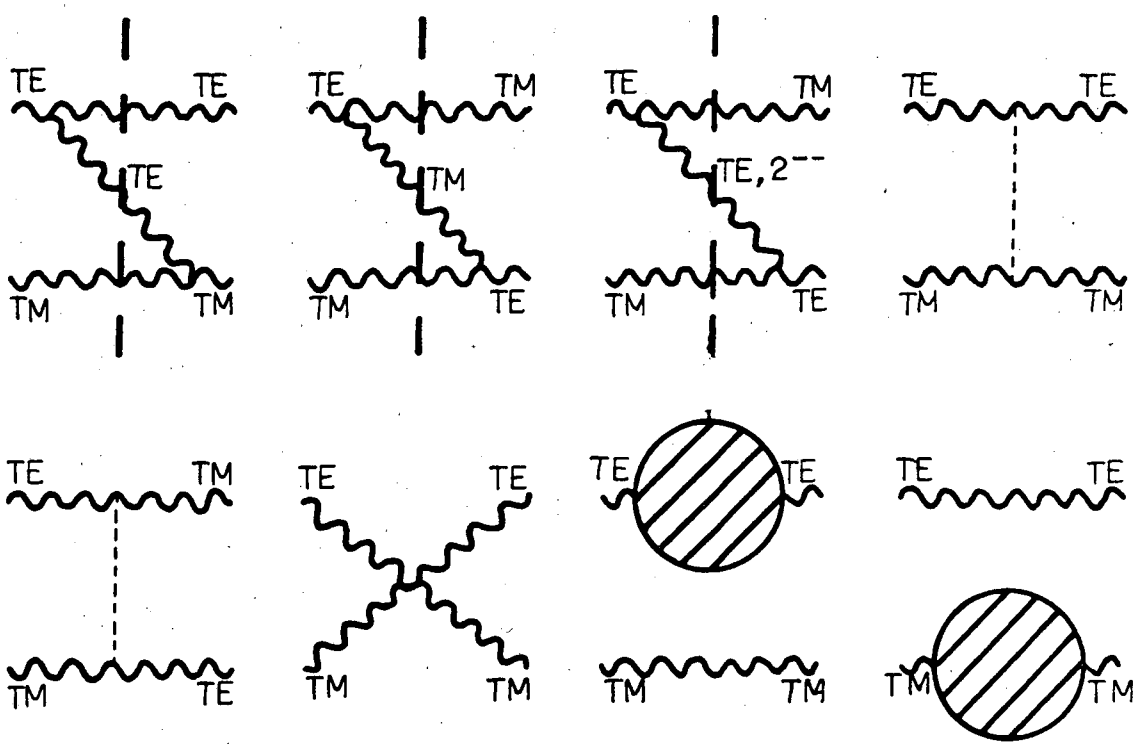
TE
TE
TE
TM
TE
TM
TM
TM
TE
TE
TM
TE,2⁻⁻
TM
TE
TE
TE
TM
TM
TE
TE
TE
TE
TE
TE
TM
TM
TM
TM
TM
TM

(b)

Figure 3

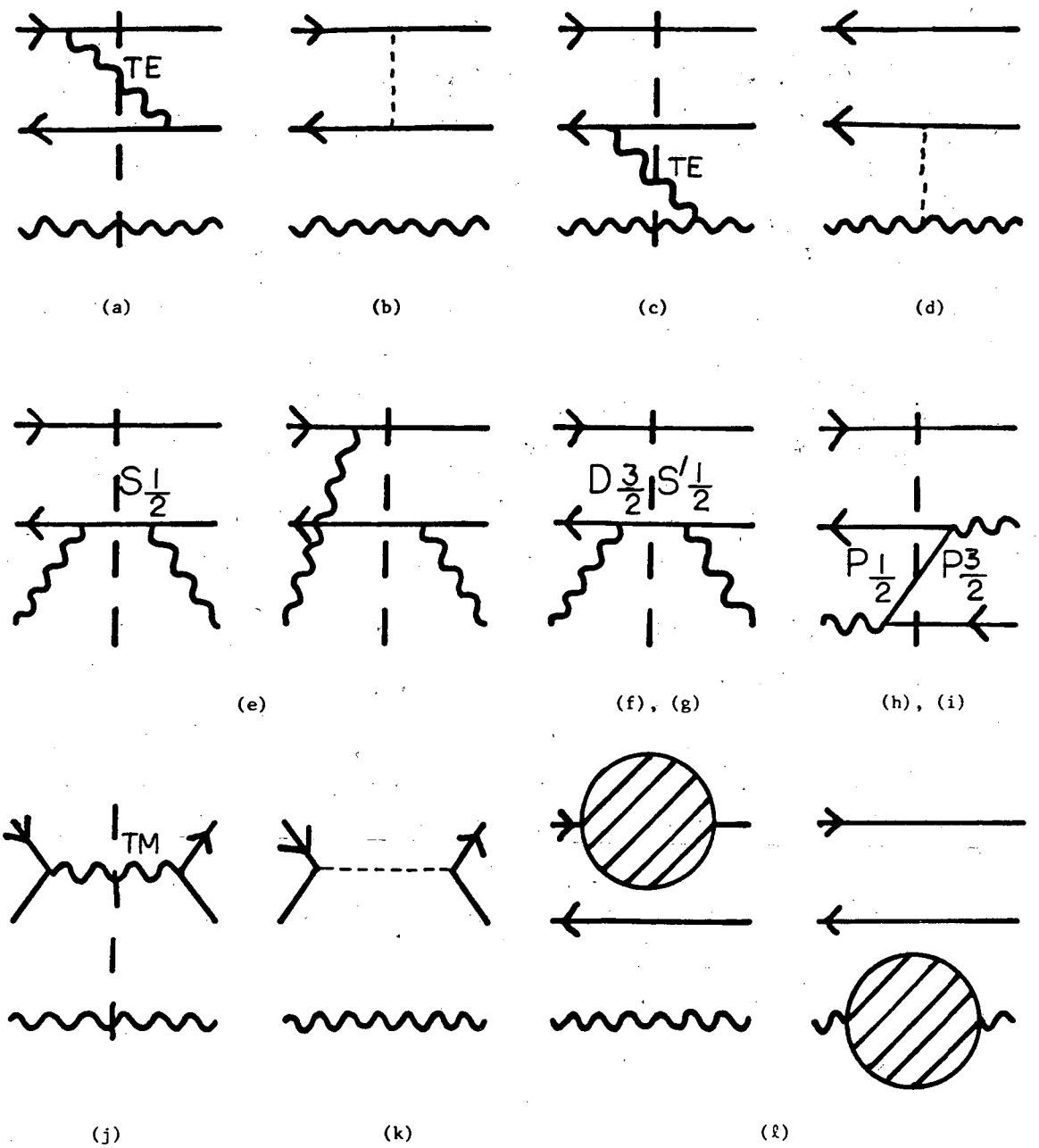
TE
TE
(a)
(b)
(c)
(d)
$S\frac{1}{2}$
$D\frac{3}{2}$ $S'\frac{1}{2}$
$P\frac{1}{2}$ $P\frac{3}{2}$
(e)
(f), (g)
(h), (i)
TM
(j)
(k)
(ℓ)

Figure 4

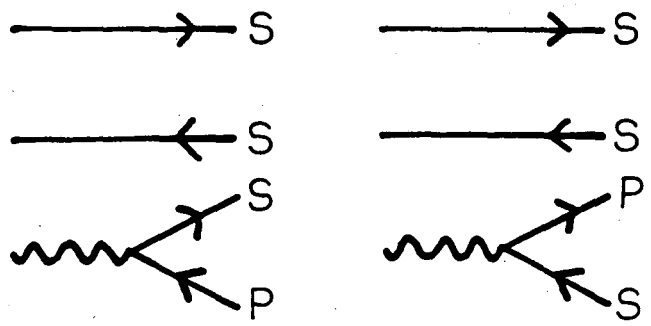

Figure 5

This report was done with support from the Department of Energy. Any conclusions or opinions expressed in this report represent solely those of the author(s) and not necessarily those of The Regents of the University of California, the Lawrence Berkeley Laboratory or the Department of Energy.

Reference to a company or product name does not imply approval or recommendation of the product by the University of California or the U.S. Department of Energy to the exclusion of others that may be suitable.

TECHNICAL INFORMATION DEPARTMENT
LAWRENCE BERKELEY LABORATORY
UNIVERSITY OF CALIFORNIA
BERKELEY, CALIFORNIA 94720